Research Paper

GEOSPHERE

GEOSPHERE, v. 18, no. 6

https://doi.org/10.1130/GES02519.1

17 figures; 1 table; 1 set of supplemental files

CORRESPONDENCE: tom.lehman@ttu.edu

CITATION: Lehman, T.M., Cobb, J., Sylvester, P., and Souders, A.K., 2022, The Cretaceous-Paleogene contact in the Tornillo Group of Big Bend National Park, West Texas, USA: Geosphere, v. 18, no. 6, p. 1851–1884, https://doi.org/10.1130/GES02519.1.

Science Editor: David E. Fastovsky

Received 31 January 2022
Revision received 20 July 2022
Accepted 18 August 2022

Published online 23 September 2022

GOLD OPEN ACCESS

THE GEOLOGICAL SOCIETY OF AMERICA®

The Cretaceous-Paleogene contact in the Tornillo Group of Big Bend National Park, West Texas, USA

Thomas M. Lehman, Jacob Cobb, Paul Sylvester, and A. Kate Souders*
Department of Geosciences, Texas Tech University, Lubbock, Texas 79409-1053, USA

ABSTRACT

The Cretaceous-Paleogene (K-Pg) contact interval is constrained by vertebrate fossil sites at seven sites in the Tornillo Group and lies within an 80–100-m stratigraphic section between the top of the Javelina Formation and the base of the "log jam sandstone" marker bed in the Black Peaks Formation. In western exposures of this interval, the highest occurrence of in situ dinosaur specimens and the lowest occurrence of Paleocene mammal specimens are separated by an unusual conglomerate bed. This thin conglomerate bed coincides with the contact between Cretaceous and Paleogene strata and contains reworked Cretaceous fossils. It is superficially similar to conglomerate beds elsewhere attributed to the effects of tsunamis generated by the Chicxulub impact; however, the maximum depositional age of ca. 63 Ma based on detrital zircons indicates that the conglomerate was deposited about three million years after the K-Pg boundary event. Paleocene mammalian fossils from immediately above the conglomerate bed represent a fauna that can be no older than the middle Torrejonian (To2 interval zone). The contact between Cretaceous and Paleocene strata is therefore disconformal and represents a hiatus of at least three million years. A condensed section occurs at the westernmost exposure of the K-Pg contact, where at least 80 m of strata are absent below the conglomerate bed; these strata are present in exposures farther east. This condensed section likely records an erosional event resulting from uplift and deformation of the nearby Terlingua monocline. Although the 80 m of strata below the conglomerate bed are poorly fossiliferous, several clearly in situ dinosaur specimens indicate that this entire interval is Late Cretaceous in age. There is no compelling evidence for preservation of the K-Pg boundary event horizon at any of the seven sites in the Tornillo Group, and so the hiatus represented at the Cretaceous/Paleocene contact here likely also includes some part of latest Cretaceous time. Mammalian specimens from sites in the "log jam sandstone," ~40 m above the middle Torrejonian sites, represent an early Tiffanian fauna (Ti1 interval zone). Latest Torrejonian (To3) sites have not been recognized, and therefore a second disconformity likely coincides with the base of the "log jam sandstone" marker horizon in the Black Peaks Formation.

■ INTRODUCTION

During the past several decades, many sites that preserve the Cretaceous-Paleogene (K-Pg) boundary horizon have been documented around the Gulf of Mexico and Caribbean (e.g., O'Campo et al., 1996; Lawton et al., 2005; Schulte et al., 2010; Denne et al., 2013) within ~1000 km radius of the Chicxulub impact crater (e.g., Gulick et al., 2019). These sites are all within marine strata. Fluvial deposits of the Tornillo Group in the Big Bend region of Texas provide the only nearby exposures of non-marine strata thought to span the K-Pg boundary in proximity to the Chicxulub impact site. Unlike well-documented sections that record the K-Pg boundary interval in continental strata within the interior in North America, however, such as in the Hell Creek and Fort Union formations in Montana and North Dakota (Hartman et al., 2002; Nichols and Johnson, 2008; Wilson et al., 2014), the Denver Basin in Colorado (Clyde et al., 2016; Fuentes et al., 2019; Lyson et al., 2019), or the San Juan Basin in New Mexico (Flynn et al., 2020). The Tornillo Group strata in the Big Bend region are folded, faulted, intruded by late Paleogene igneous rocks, and extensively covered by Neogene and Quaternary alluvium (Fig. 1; Lehman et al., 2018). As a result, stratigraphic relationships within the Tornillo Group are in many areas not easily determined. Moreover, the K-Pg contact interval in Big Bend is only sparsely fossiliferous. So, although the interval spanning the contact between Upper Cretaceous and Paleocene strata here has been studied since the 1960s, it remains unclear how complete the stratigraphic section may be, and whether or not the impact horizon itself is preserved.

The purpose of the present study is to document the nature of the contact between Cretaceous and Paleocene strata at all sites in the Tornillo Group where fossils allow this interval to be narrowly constrained stratigraphically. One of these sites, on Dawson Creek at the western edge of Big Bend National Park, has been a subject of intensive study for several decades, and so is already well documented. However, the section exposed on Dawson Creek is in many ways not typical of exposures found elsewhere in the Tornillo Group; therefore, it is useful to record the stratigraphic relationships found in other nearby areas as well.

In this study, the stratigraphic positions of all significant Cretaceous and Paleocene vertebrate fossil sites within the K-Pg contact interval are

*Present address: Geology, Geophysics, and Geochemistry Science Center, U.S. Geological Survey, Denver, Colorado 80225, USA

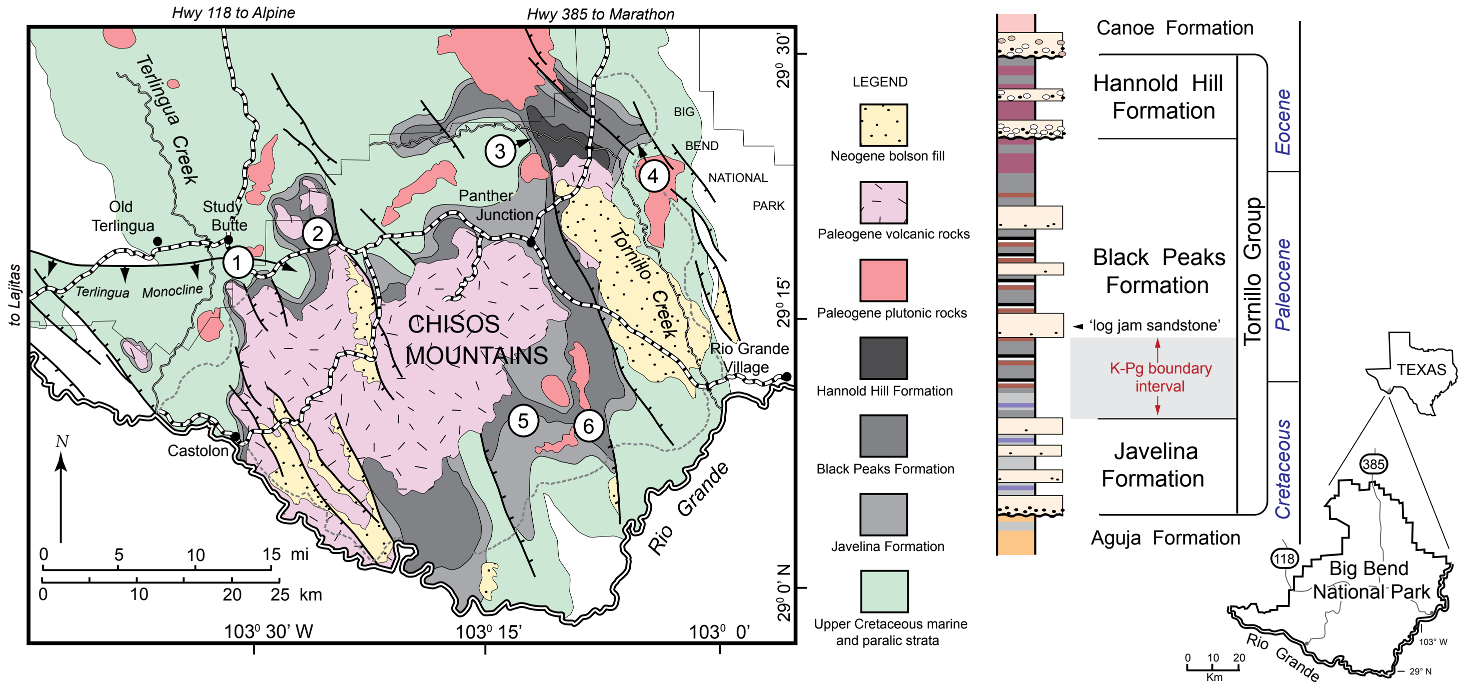

Figure 1. Generalized geologic map of the Big Bend region in Texas (modified from Turner et al., 2011) showing regional extent of the Tornillo Group, its relationship to surrounding geologic features, and the location of exposures discussed in the text: (1) Dawson Creek; (2) Rough Run Creek; (3) Grapevine Hills; (4) McKinney Hills; (5) Robber's Roost; and (6) Glenn Draw. Shown (right) is an index map with location of Big Bend National Park and a generalized stratigraphic section of the Tornillo Group showing contacts between its constituent formations given by Lehman et al. (2018) and the Cretaceous-Paleogene (K-Pg) contact interval described in the present study.

documented for seven areas where this stratigraphic interval is exposed. At several of these sites, the contact between Cretaceous and Paleocene strata is found to coincide with an unusual thin conglomerate bed. This bed contains a reworked Upper Cretaceous charophyte algal flora, but it lacks exotic components such as microspherules elsewhere attributed to the K-Pg boundary impact event. An assemblage of detrital zircons obtained from the conglomerate bed is shown to yield a U/Pb maximum depositional age (MDA) estimate of ca. 63 Ma. The mammalian fauna found in lowermost Paleocene strata at all sites is shown to be of middle Paleocene (Torrejonian) age, compatible with the MDA of ca. 63 Ma. Collectively, data presented in this study therefore indicate that the contact between Upper Cretaceous and Paleocene strata in the Tornillo Group is disconformal and represents a hiatus of at least 3 million years. Although the term "K-Pg contact interval" is used herein to denote the stratigraphic interval that encompasses the contact between Upper Cretaceous and Paleocene strata, data presented herein indicate that the K-Pg event bed (impact horizon), and thus the actual K-Pg boundary itself, is not preserved in the Tornillo Group.

BACKGROUND

A historical account of the varied interpretations of the K-Pg contact in the Tornillo Group was given by Lehman et al. (2018) and is briefly summarized here. As part of the original mapping of the Tornillo Group in Big Bend National Park (hereafter "the Park") during the late 1950s to early 1960s, an attempt was made to locate the K-Pg contact on the basis of fossil content, and the formational contact between the Javelina and Black Peaks formations was placed so as to coincide with the K-Pg contact (Fig. 1). However, fossils are so scarce in these strata that it was not possible to locate the formation contact accurately on this basis in most exposures. Even so, it was believed that the Javelina Formation was entirely Cretaceous in age, and the overlying Black Peaks Formation was entirely Paleocene in age, although there were no obvious lithologic criteria that allowed for identification of the K-Pg contact. Because the lowermost Paleocene vertebrate fossils recovered at that time from the Black Peaks Formation represented a Torrejonian (North American Land Mammal Age) fauna of middle Paleocene age, the Javelina-Black Peaks formational contact was thought to be unconformable (e.g., Maxwell et al., 1967). Up to the early 1970s, it was generally believed that earliest Paleocene (Puercan) strata were absent in the Tornillo Group and either never deposited or eroded away prior to middle Paleocene time.

During the 1970s and 1980s, however, it was found that the K-Pg contact does not coincide with the position of the Javelina–Black Peaks formational contact as depicted on maps available at that time (Maxwell et al., 1967; Lehman, 1985). A Paleocene mammalian assemblage was discovered at a site (known as "Tom's Top") in strata mapped as the upper Javelina Formation on Dawson Creek (Lawson, 1972; Fig. 2). Another locality in the Javelina Formation (referred to as the "Dogie" site) nearby on Rough Run Creek also yielded a Paleocene mammalian fauna (Standhardt, 1986; Fig. 2). This suggested that the K-Pg contact was somewhere within the upper part of the Javelina Formation, at least as those strata were mapped on the western side of the Park. The fossil mammals collected at the "Tom's Top" and "Dogie" sites were interpreted to be of late Puercan age (Standhardt, 1986; Schiebout et al., 1987) but the sites are ~40–80 m, respectively, above the highest occurrence of dinosaur bones in those areas, leaving open the possibility that undiscovered earlier Paleocene sites might exist in the intervening section.

In the 1990s, an attempt was made to locate the iridium abundance anomaly, tsunami bed, or any other physical or chemical evidence for the K-Pg impact event in the exposures on Dawson Creek. A very weak iridium abundance anomaly was detected, but no compelling evidence for the impact horizon was discovered (Lehman, 1990). Even so, throughout the 1990s, it was generally believed that no unconformity was present in the section, and that latest Cretaceous (Lancian) and early Paleocene (Puercan) vertebrate faunas are present within these strata, although no evidence for the K-Pg impact horizon was found (Standhardt, 1986; Schiebout et al., 1987, 1988; Lehman, 1988).

During the 2000s, the formation contacts within the Tornillo Group were revised, and these strata were mapped more accurately throughout

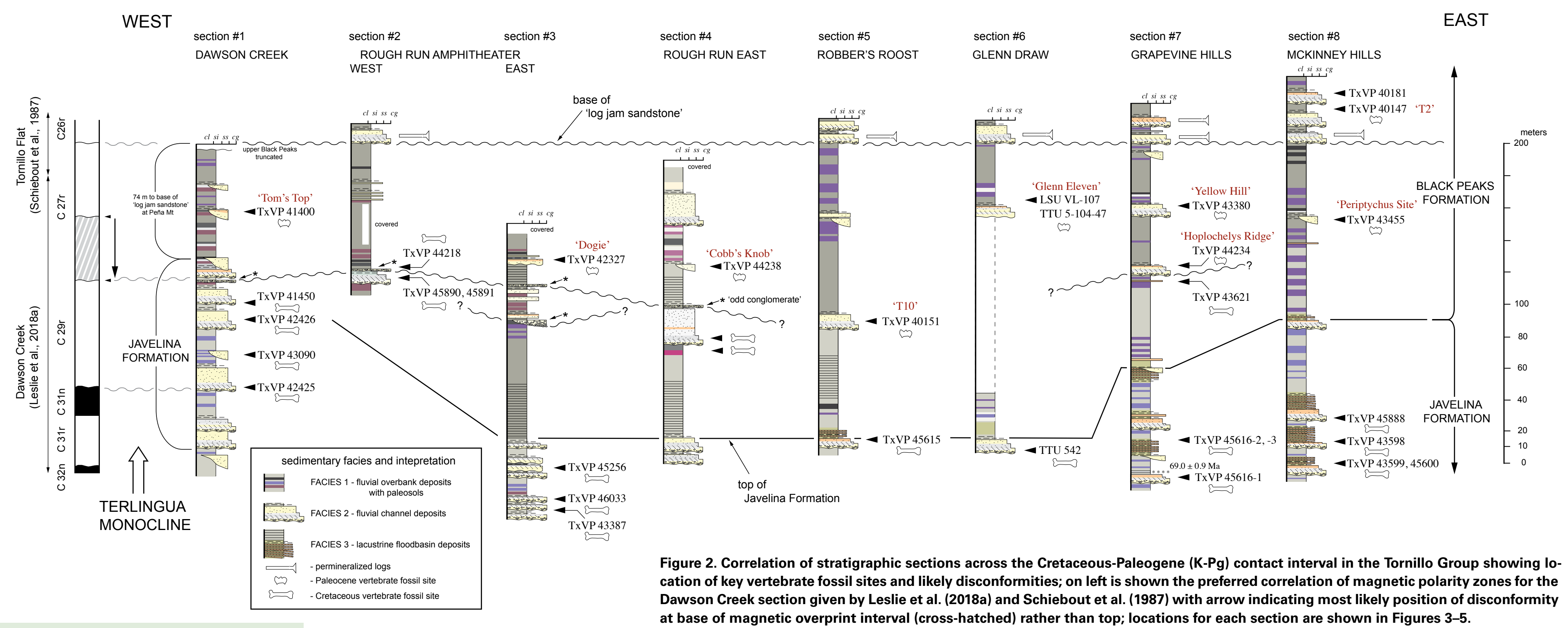

Figure 2. Correlation of stratigraphic sections across the Cretaceous-Paleogene (K-Pg) contact interval in the Tornillo Group showing location of key vertebrate fossil sites and likely disconformities; on left is shown the preferred correlation of magnetic polarity zones for the Dawson Creek section given by Leslie et al. (2018a) and Schiebout et al. (1987) with arrow indicating most likely position of disconformity at base of magnetic overprint interval (cross-hatched) rather than top; locations for each section are shown in Figures 3–5.

the Big Bend region (Lehman, 2002, 2004, 2007). The Javelina-Black Peaks formational contact was revised to coincide with more easily recognizable lithologic criteria, rather than fossil content. The most recent geologic map of Big Bend Park (Turner et al., 2011) uses this revised contact, and where it is possible to identify the K-Pg contact interval, it is everywhere within the lowermost part of the Black Peaks Formation, at or just above its contact with the Javelina Formation, and below the "log jam sandstone," a distinctive marker bed within the lower part of the Black Peaks Formation (Lehman et al., 2018).

Most recently, Cobb (2016) documented an unusual conglomerate bed at the K-Pg contact on Rough Run Creek; he interpreted this bed as a tsunami deposit resulting from the Chicxulub impact, and Wiest et al. (2018) purported to identify the K-Pg boundary at the exposure on Dawson Creek on the basis of a stratigraphic change in the diameter of burrows within the fluvial sediments. Leslie et al. (2018a) obtained a paleomagnetic polarity sequence for the section on Dawson Creek and provided $^{40}Ar/^{39}Ar$ ages for detrital sanidine from sandstone beds throughout the section there. They also determined that the mammalian fossils from both the "Tom's Top" and "Dogie" localities are actually middle Torrejonian rather than late Puercan in age, and that at least on Dawson Creek, a disconformity separates middle Torrejonian strata from underlying strata thought to span the K-Pg boundary.

Altogether, there are seven localities within the Tornillo Group where the stratigraphic position of the K-Pg contact can be constrained on the basis of vertebrate fossils (Figs. 1 and 2). At six of these seven localities, the geological setting and stratigraphic levels of key paleontological sites straddling the K-Pg contact interval have for the most part not been documented. Only the section on Dawson Creek has received detailed study. The present report provides an account of the geological setting and stratigraphy at each of the seven sites, describes the Paleocene mammalian fossils recovered for those sites not already well documented, and presents additional age constraints based on $^{206}Pb/^{238}U$ ages for detrital zircons from several key beds within the K-Pg contact interval.

METHODS

Geologic maps were prepared to document each of the seven areas where Cretaceous and Paleocene vertebrate fossil sites constrain the position of the K-Pg contact interval to a relatively narrow stratigraphic section (Lehman, 2002, 2004, 2007; Cobb, 2016). Stratigraphic sections of the K-Pg contact interval were measured at each of the seven areas, and a series of detailed stratigraphic sections were taken in one area to document lateral variability in the "odd conglomerate" bed (Rough Run East locality; Cobb, 2016). Mammalian fossils were collected by surface-picking during multiple visits to each of the sites; specimens were photographed using an AmScope MT Series microscope camera and Olympus model SCXZ binocular microscope. A sample consisting of ~65 charophyte algal gyrogonites was collected by hand-picking a washed sand sample from the "odd conglomerate" bed and was photographed using the same camera and microscope.

Bulk sand samples from the matrix of the "odd conglomerate" and from the sandstone bed at its top were processed and examined to determine if components elsewhere associated with the K-Pg impact horizon (e.g., microspherules and "shocked" quartz grains) could be identified here. The bulk samples were disaggregated and dried, soaked in kerosene (K1), washed with hot water, and sieved using a 230 mesh (62 micron) sieve to remove silt and clay-sized particles. The resulting sand concentrate was examined using a binocular microscope to select grains with spherical form or with planar or lamellar surface micro-textures. Approximately 122 grains were hand-picked for detailed examination using scanning electron microscopy (SEM) and energy-dispersive spectrum (EDS) analysis. The grains were mounted on an aluminum stub with double-coated carbon paper, and sputter coated with gold-palladium. The Hitachi S4300 SEM with tungsten filament was set at 15 kV accelerating potential, brightness value 1, and EDS to assess chemical composition of the grains (Cobb, 2016).

Samples of the "odd conglomerate" (JC 8) and two mudstone beds (KT4 and KTTb) within the K-Pg contact interval were collected to assess their maximum depositional ages based on $^{206}Pb/^{238}U$ age determination for detrital zircons. Zircons were separated from the three samples using heavy liquid methylene iodide (3.32 g/cm^3) and hand-picking, mounted in epoxy, and imaged by SEM using backscattered electrons (BSE). Zircons in JC 8 were also imaged by SEM-based cathodoluminescence (CL). Small numbers of detrital zircons were dated for U/Pb age by laser ablation–inductively coupled plasma–mass spectrometry (LA-ICP-MS) for samples KT4 (n = 25) and KTTb (n = 41) at University of California, Santa Barbara, in 2013. Measurements were made using a Nu Instruments HR Nu Plasma multicollector-ICP-MS coupled to a Photon Machines 193nm ArF excimer laser and a 24 µm ablation spot. Spots were placed near grain margins, where possible, in order to date the youngest magmatic age recorded by the zircon, but fractures and metamict damage were observed in the rims of many grains; therefore, in these cases, spots were placed somewhat toward the grain interiors.

For sample JC 8, a large number of detrital zircons (n = 133) were dated by LA-ICP-MS in the Mineral Isotope Laser Laboratory (MILL) at Texas Tech University in 2019. Measurements were made using a Nu Instruments AttoM single collector-ICP-MS coupled to an ESI NWR 193nm ArF excimer laser and a 20-µm ablation spot. Unlike samples KT4 and KTTb, zircon grain quality was good (fracture-poor) even in the rims of a large majority of grains; so ablation spots were placed at the rims for almost all analyses. LA-ICP-MS U-Pb data for all three samples and zircon standard reference materials (SRMs) are presented in Tables S1–S3[1] in the Supplemental Material. Wetherill U/Pb concordia diagrams for the three samples and zircon secondary SRMs are presented in Figures S1 and S2, respectively, of the Supplemental Material. Age distributions of the detrital zircons in each of the three samples are shown in combined histogram–kernel density estimation (KDE) plots in Figure 16. Maximum depositional age (MDA) estimates were

[1]Supplemental Material. Table S1: LA-ICP-MS U-Pb zircon data. Figure S1: Wetherill U-Pb concordia diagrams for detrital zircons. Figure S2: Wetherill U-Pb concordia diagrams for zircon standard reference materials. Please visit https://doi.org/10.1130/GEOS.S.20514117 to access the supplemental material, and contact editing@geosociety.org with any questions.

obtained by two methods: using the age and uncertainty of the youngest grain measured within the sample (e.g., Dickinson and Gehrels, 2009), and using the weighted average of the youngest three ages that overlap with 2σ uncertainty (e.g., Zhang et al., 2016).

Throughout the following text, for ease of communication, the significant vertebrate fossil sites are referred to by names (e.g., "Tom's Top" and "Dogie") recorded in the Texas Vertebrate Paleontology Collections register at the Jackson School Museum of Earth Sciences, as well as their corresponding locality numbers (e.g., TxVP 41400 and TxVP 42327).

Abbreviations used in this paper: TxVP—Texas Vertebrate Paleontology Collections at the Jackson School Museum of Earth Sciences, University of Texas at Austin (formerly collections of the Texas Memorial Museum, and so the acronym TMM has previously been used for all of the same sites and specimens now identified with the TxVP acronym), LSU—Louisiana State University Museum of Geology, Baton Rouge, Louisiana.

GEOLOGIC SETTING

In each of the seven areas where Cretaceous and Paleocene vertebrate fossil sites constrain the position of the K-Pg contact interval, it lies within or just above the boundary between the Javelina Formation and Black Peaks Formation (Figs. 3–5 and Appendix).

The Javelina Formation includes a succession of prominent cliff-forming conglomeratic sandstone beds that weather to form erosionally resistant ridges (Turner et al., 2011; Lehman et al., 2018). The upper contact of the formation is placed at the top of the highest of these ridge-forming sandstone beds (Fig. 2). Because the individual sandstone beds are laterally discontinuous where traced over several kilometers, this contact is gradational and intertonguing over a stratigraphic interval of as much as 20 m.

The lower 80–100 m of the Black Peaks Formation consist primarily of slope-forming multicolored mudstone with lenticular sandstones that in most cases cannot be traced laterally beyond a kilometer, and do not weather to form resistant ridges. The lowest prominent cliff-forming sandstone beds in the Black Peaks comprise a distinctive marker horizon referred to informally as the "log jam sandstone" (Lehman et al., 2018). This sandstone interval typically consists of two sandstone beds, both of which contain abundant large, permineralized logs (Wheeler, 1991; Lehman and Busbey, 2007); as a result this interval is readily recognizable, and can be correlated throughout the Big Bend region (Fig. 2).

In all seven of the exposures described below, the K-Pg contact interval therefore lies within a slope-forming section composed predominantly of multicolored mudstone between the top of the Javelina Formation and the base of the "log jam sandstone" in the Black Peaks. This section varies from ~80–140 m in thickness, and within it, there are only a few key beds that can be traced beyond the limits of a given outcrop. One of the marker horizons within the K-Pg contact interval is a peculiar bed referred to informally as the "odd conglomerate" and described by Lehman and Busbey (2007) and Cobb (2016). A more detailed account of the "odd conglomerate" is given in the present report. It has thus far been recognized only in western exposures of the K-Pg contact interval in the Park, where it appears to coincide with a disconformity separating Cretaceous and Paleocene strata.

There are three broad sedimentary facies associations represented in these strata; referred to herein as Facies 1, 2, and 3 (in order of relative abundance from greatest to least; Fig. 2). These facies have been thoroughly described by previous authors cited below, and so a detailed account is unnecessary here. Facies 1 consists primarily of unstructured, multicolored mudstone with horizons of interstitial calcium carbonate nodules and subordinate lenses of thinly bedded siltstone and very fine-grained sandstone. These facies are interpreted to represent well-drained fluvial overbank flood-plain deposits with paleosol horizons ("overbank-association facies" of Atchley et al., 2004; see also Lehman, 1989, 1990; Vines, 2000; Nordt et al., 2003, 2011; White and Schiebout, 2003, 2008; Schmidt, 2009; Bataille et al., 2016, 2019). Facies 2 consists of thickly bedded, cross-stratified, conglomeratic fine- to medium-grained sandstone in fining-upward successions. These facies are interpreted to represent fluvial channel deposits ("channel-association facies" of Atchley et al., 2004; see also Lawson, 1972; Lehman, 1985, 1991, 2021; Straight, 1996; Bataille et al., 2019). Facies 3 consists primarily of rhythmically bedded, bioturbated, calcareous siltstone and mudstone. These facies are interpreted to represent lacustrine flood-basin and abandoned channel deposits (Schmidt, 2009; Lehman, 2021).

Dawson Creek

The best exposed and most thoroughly studied outcrop of the K-Pg contact interval is along the western edge of the Park, on the south side of Dawson Creek (Fig. 3). Of the seven areas where the K-Pg contact interval can be constrained with vertebrate fossil sites, the Dawson Creek area is the only one that has been well documented geologically (Lawson, 1972; Standhardt, 1986; Lehman, 1990; Leslie et al., 2018a). The section here spanning the K-Pg contact has been a subject of a variety of studies including fluvial sedimentology (Atchley et al., 2004), paleoclimatology (Nordt et al., 2003), and paleosol geochemistry (Nordt et al., 2011).

The Javelina Formation on Dawson Creek is very fossiliferous, and has yielded a variety of significant Cretaceous vertebrate fossils, including the holotype specimen of the giant pterodactyl *Quetzalcoatlus northropi* (TxVP 41450-3; see Appendix; Fig. 2). Other sites have produced isolated limb bones and vertebrae of *Alamosaurus sanjuanensis* (TxVP 42425, 42426, and 43090). The highest Cretaceous vertebrate fossil specimen recovered here (TxVP 44219-1, a tyrannosaurid tooth) was collected ~2 m below the "odd conglomerate" bed (Fig. 2), although its isolated occurrence and abraded condition leave open a possibility that the specimen may have been exhumed and reworked prior to burial. Until recently, the "odd conglomerate" bed had been overlooked or not identified by previous workers in the Dawson Creek exposure. Although it is very thin, obscure, and mostly covered by colluvium (Fig. 6C), the "odd conglomerate" is present

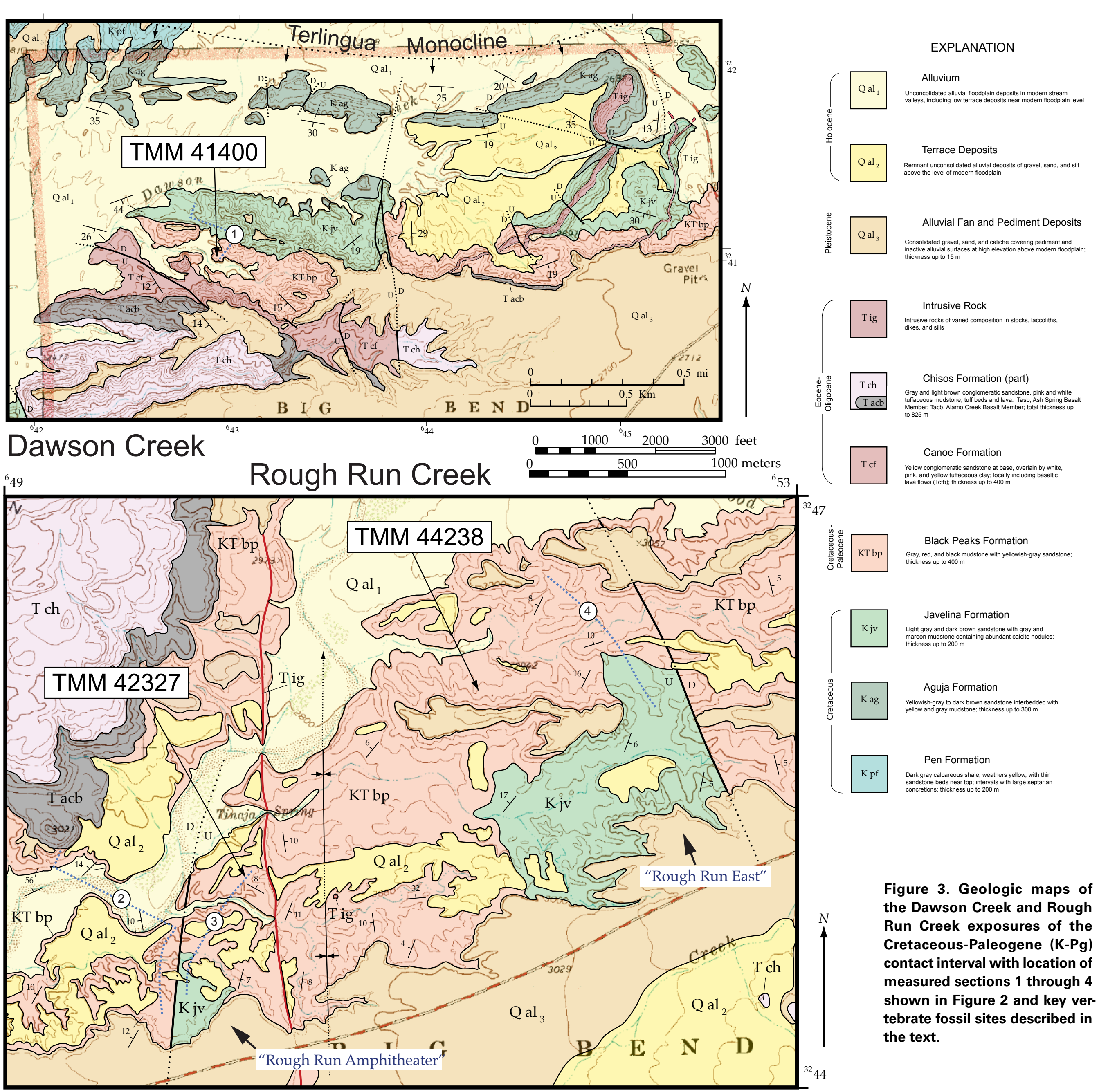

Figure 3. Geologic maps of the Dawson Creek and Rough Run Creek exposures of the Cretaceous-Paleogene (K-Pg) contact interval with location of measured sections 1 through 4 shown in Figure 2 and key vertebrate fossil sites described in the text.

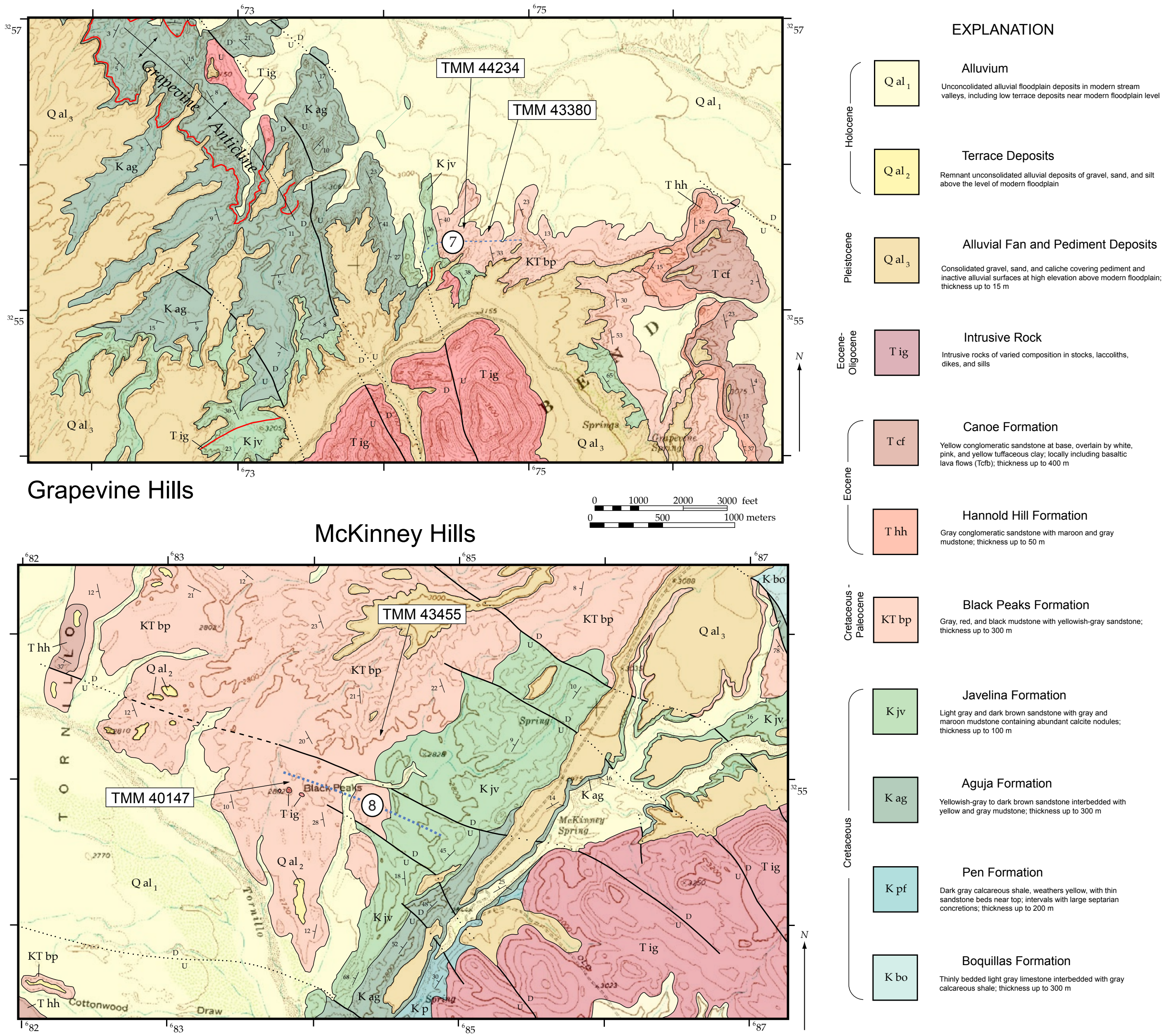

Figure 4. Geologic maps of the Grapevine Hills and McKinney Hills exposures of the Cretaceous-Paleogene (K-Pg) contact interval with location of measured sections 7 and 8 shown in Figure 2 and key vertebrate fossil sites described in the text.

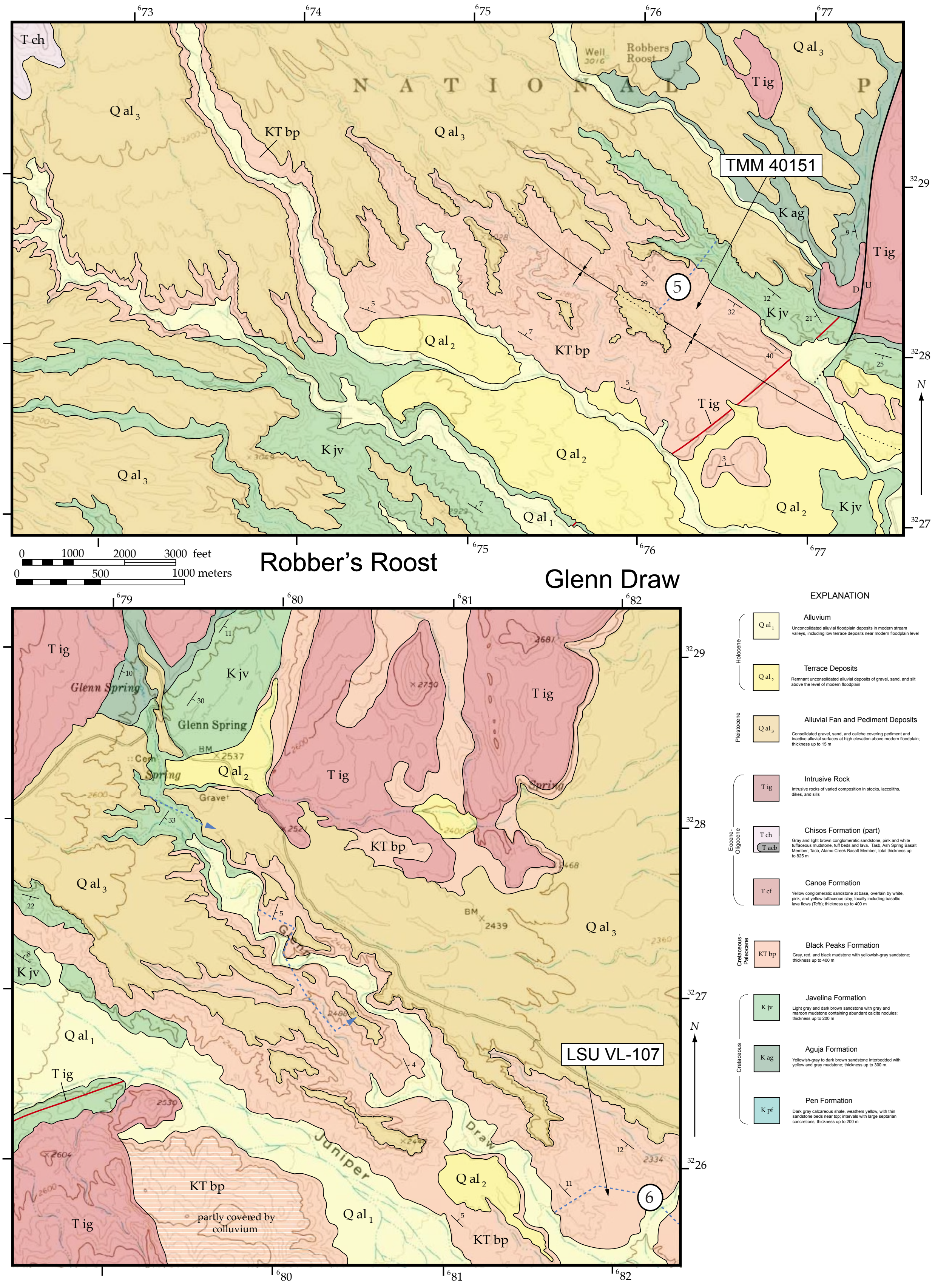

Figure 5. Geologic maps of the Robber's Roost and Glenn Draw exposures of the Cretaceous-Paleogene (K-Pg) contact interval with location of measured sections 5 and 6 shown in Figure 2 and key vertebrate fossil sites described in the text.

Figure 6. Photographs showing the Cretaceous-Paleogene (K-Pg) contact interval on Rough Run Creek and Dawson Creek: (A) Rough Run Amphitheater East (section #3 of Fig. 2) showing two facies of "odd conglomerate" bed with Facies A—thin bed with poorly sorted, matrix-supported texture and Facies B—thick lenticular bed with stratified, grain-supported texture; (B) view immediately east of image A showing thin bed of "odd conglomerate" (white arrows) in relationship to the "Dogie" locality; (C) Dawson Creek exposure (section #1 of Fig. 2) showing Facies A of "odd conglomerate" bed resting on irregular erosional surface (white arrows); (D) view immediately west of image C showing large "outsized" clasts in "odd conglomerate" (white arrow); (E) detailed view of area in image D showing typical outcrop appearance of Facies A in the "odd conglomerate" bed; (F) Rough Run East exposure (section #4 of Fig. 2) showing northeastern margin of paleo-valley floored by "odd conglomerate" bed (white arrows); (G) detailed view of "odd conglomerate" (white arrows) Facies A with outsized clasts in area shown along left side of image F; (H) stratified Facies B of "odd conglomerate" at Rough Run East exposure (section #7 of Fig. 8).

here just above the mudstone bed from which TxVP 44219-1 (the isolated tyrannosaurid tooth) was collected, and 15 m above the base of the sandstone bed from which the *Quetzalcoatlus northropi* holotype was recovered (Fig. 2).

The "Tom's Top" site (TxVP 41400) is 40 m above the "odd conglomerate," within the lowermost part of the Black Peaks Formation. The mammalian fauna recovered at Tom's Top was initially interpreted to be late Puercan in age by Standhardt (1986) and Schiebout et al. (1987), but Leslie et al. (2018a) showed that it is instead middle Torrejonian (To2; see also Williamson, 1996; Lehman and Busbey, 2007). Although there are Paleocene vertebrate fossil sites both lower (TxVP 44235) and higher (LSU VL-109) than Tom's Top, these other sites have yet to yield biostratigraphically useful mammalian specimens. The 40 m interval between the highest in situ dinosaur bones and the Tom's Top site on Dawson Creek has thus far yielded no useful fossils. The upper part of the Black Peaks Formation here was truncated by erosion prior to middle Eocene time, and is overlain by the Canoe Formation (Lehman et al., 2018). A section exposed nearby at Peña Mountain is, although unfossiliferous, more complete, and the thickness of the interval between the top of the Javelina Formation and base of the "log jam sandstone" there is 74 m (Lehman et al., 2018; their section #22). It is assumed that this interval would have been roughly comparable in thickness at Dawson Creek prior to Eocene erosion (Fig. 2).

Rough Run Amphitheater

The K-Pg contact interval is also exposed ~8 km east of Dawson Creek, in a broad amphitheater-like expansion on the southern side of the valley of Rough Run Creek (Fig. 3). This is where the "Dogie" locality (TxVP 42327) described by Standhardt (1986), Schiebout et al. (1987), and Leslie et al. (2018a) is found, but the section here is more difficult to interpret. The Rough Run Amphitheater exposure is cut by at least one major north-trending fault, and interrupted by a dike along the eastern margin. Pleistocene pediment gravel covers much of the Javelina and Black Peaks formations, and vegetated Holocene stream terraces obscure relationships between adjacent exposures (Fig. 3). These complications make it difficult to confidently determine stratigraphic relationships in this area.

On the west side of the fault, only the lower part of the Black Peaks Formation is exposed (Fig. 2, section #2). An extensive sandstone bed here has yielded abundant specimens of the sauropod dinosaur *Alamosaurus sanjuanensis* (e.g., TxVP 45890, 45891; Fronimos and Lehman, 2014). The highest in situ dinosaur specimen collected here on the west side of the fault (TxVP 44218-1, an isolated tyrannosaurid tooth) was found in a conglomerate bed just above the *Alamosaurus*-bearing interval, although its fragmentary condition suggests that the specimen may have been exhumed and reworked prior to burial (Fig. 2, section #2). Above this conglomerate is a distinctive multicolored series of mudstone layers with alternating black, red, and light-gray bands. Such beds are only known to occur in the Paleocene part of the Black Peaks Formation in other areas of the Park. The K-Pg contact may therefore be at or near the base of the variegated mudstone interval here, but thus far no diagnostic Paleocene fossils have been found anywhere on the west side of the fault (Lehman and Busbey, 2007). The "log jam sandstone" bed is exposed nearby on the north bank of Rough Run Creek, and so the sites west of the fault can be placed in the section relative to this marker bed (Fig. 2, section #2).

In contrast, east of the fault, the upper part of the Javelina Formation is exposed up to its contact with the Black Peaks Formation, and a significant section of the lower Black Peaks Formation extends up to a north-trending dike (Fig. 3). The upper part of the Javelina Formation here has produced a wide variety of dinosaur specimens including the holotype of ?*Gryposaurus alsatei* (TxVP 46033-1, Lehman et al., 2016), as well as fishes, turtles, and crocodylians (TxVP 43678; the "Bowfin Beach" site described by Standhardt, 1986; Lehman and Busbey, 2007). The uppermost sandstone interval in the Javelina Formation here has thus far produced only a single isolated pterodactyl bone (TxVP 45256-1). The Javelina-Black Peaks formation contact is placed at the top of this sandstone interval. The "Dogie" site (TxVP 42327) is ~110 m above the top of the Javelina Formation here (Fig. 2, section #3). This site has produced a middle Torrejonian (To2) mammalian fauna (Williamson, 1996; Leslie et al., 2018a). The intervening part of the section has yielded no significant fossils but is marked here also by the unusual "odd conglomerate" bed.

In summary, the uppermost in situ Cretaceous fossil locality in the Rough Run Amphitheater area is found west of the fault, but the lowermost Paleocene fossil locality is found east of the fault, and correlation of key stratigraphic units on opposite sides is uncertain (Fig. 2, sections #2 and #3). Although the peculiar "odd conglomerate" bed is well exposed east of the fault, the distinctive *Alamosaurus*-bearing sandstone bed is not present here. Moreover, there are no nearby exposures of the "log jam sandstone" marker bed, and so the total thickness of the K-Pg contact interval east of the fault can only be estimated.

Rough Run East

About 3 km east of the Rough Run Amphitheater, the same stratigraphic interval is exposed, however, here dipping gently to the northwest with minimal structural complexity and with less extensive cover by Pleistocene and Holocene alluvium (Fig. 3). This exposure was referred to by Cobb (2016) as the "Rough Run East" outcrop. The "odd conglomerate" bed is much more laterally extensive here, widely exposed throughout this area, and its stratigraphic position within the K-Pg contact interval is clear (Fig. 2, section #4; see below). The highest in situ Cretaceous vertebrate fossil site here consists of a complete titanosaur limb bone (Fig. 2, section #4). This specimen remains in place. Parts of additional titanosaur bones exposed in the overlying sandstone unit (Fig. 2, section #4) also remain uncollected but may have been reworked. The lowest Paleocene vertebrate fossil site here, TxVP 44238 ("Cobb's Knob"), has thus far yielded two mammalian specimens (described below).

Grapevine Hills

The K-Pg contact interval northwest of Grapevine Hills is exposed along the east limb of the

"Grapevine anticline" and strata here dip steeply to the east (Fig. 4; Straight, 1996; Lehman et al., 2018). The stratigraphic succession here is uncomplicated (Fig. 2, section #7). This outcrop is the site of a tuff bed within the middle of the Javelina Formation that yielded a U/Pb age of 69.0 ± 0.9 Ma (Lehman et al., 2006). Several fragmentary pterosaur specimens were recovered from the upper Javelina Formation here (e.g., TxVP 45616-2 and TxVP 45616-3), and the partial skeleton of a juvenile *Alamosaurus sanjuanensis* (TxVP 43621-1; Lehman and Coulson, 2002) was collected from the Black Peaks Formation, 2 m below the lowest Paleocene vertebrate fossil site in this area ("Hoplochelys Ridge," TxVP 44234). A second, more fossiliferous Paleocene site ("Yellow Hill," TxVP 43380) occurs 40 m higher in the section. Both Paleocene sites are substantially below the base of the "log jam sandstone" (Fig. 2, section #7).

McKinney Hills

Strata within the K-Pg contact interval north of McKinney Hills dip gently to the northwest, and although partly covered by alluvium and interrupted by several faults, the stratigraphic relationships here are straightforward (Fig. 4). This exposure was initially described by Wilson (in Maxwell et al., 1967), who documented what he interpreted as a Torrejonian mammalian fauna recovered from a site referred to as "T2" (= TxVP 40147) in the Black Peaks Formation. This site is on the eastern side of Tornillo Flat near the actual Black Peaks from which the formation name is derived (Fig. 4). A second Paleocene site (TxVP 43455, "Periptychus Site") ~70 m lower in the section here has thus far yielded a single mammalian specimen, and although the lowermost part of the Black Peaks Formation is partly covered by alluvium, this second site is 60 m above the top of the Javelina Formation. Several specimens of *Alamosaurus sanjuanensis* (TxVP 43598-1, 43599-1, and 43600-1) and *Quetzalcoatlus* sp. (TxVP 45888-2) were collected from the upper Javelina in this area (Fig. 2, section #8).

Wilson (in Maxwell et al., 1967) indicated that the "T2" site was 43 m above the base of the Black Peaks Formation as it was mapped at that time. Using the current formation contacts shown by Turner et al. (2011) and described by Lehman et al. (2018), the "T2" site is 130 m above the base of the formation and lies between two sandstone beds in the "log jam sandstone" marker horizon. Exposures of the Black Peaks Formation on western Tornillo Flat (~7 km northwest of the McKinney Hills outcrop) are much more fossiliferous, yielded the bulk of the Tiffanian mammalian fauna described by Wilson (in Maxwell et al., 1967) and Schiebout (1974), and have been the subject of numerous other studies (Rapp et al., 1983; Schiebout et al., 1987; Bataille et al., 2016); however, no fossil sites within the K-Pg contact interval have been discovered in the western Tornillo Flat area.

Robber's Roost

The exposure near Robber's Roost (Fig. 5) was briefly discussed by Wilson (in Maxwell et al., 1967) who described a single Paleocene mammalian specimen (TxVP 40151-1) recovered from a site there referred to as "T10" (= TxVP 40151), estimated to be 23 m above the base of the Black Peaks Formation as it was mapped at that time. Schiebout (1974) and Standhardt (1986) also investigated the site, and although no additional specimens were collected, they concurred with Wilson that the site was of Torrejonian age. A ceratopsian cervical bar (TxVP 45615-1) collected from the uppermost sandstone in the Javelina Formation is stratigraphically the highest Cretaceous specimen collected in this area. Using the formation contacts recognized by Turner et al. (2011) and Lehman et al. (2018, their section #16) the "T10" site (TMM 40151) is 75 m above the base of the Black Peaks Formation (Fig. 2, section #5).

Glenn Draw

Exposures in Glenn Draw, south of Glenn Spring, were initially studied by Langston in 1947 (Langston et al., 1989), who collected a femur of *Alamosaurus sanjuanensis* (TTU 542; Wick and Lehman, 2014) from the Javelina Formation there and a baenid turtle shell (TTU 5-104-47; Lawson, 1972; Tomlinson, 1997) from a Paleocene site in the lower Black Peaks Formation (Fig. 5). Standhardt (1986) later investigated the Paleocene site here (referred to as "Glenn Eleven" = LSU VL-107) and recovered fragments of two teeth (LSU V-1156 and -1157; referred to *Triisodon quivirensis* by Leslie et al., 2018a) indicative of Torrejonian age for this site. Extensive alluvial cover prevents measuring the full thickness of the lower Black Peaks Formation here (Fig. 5). It is possible, however, to determine that the "Glenn Eleven" site is ~37 m below the "log jam sandstone" (Fig. 2, section #6).

RESULTS

Contact between Cretaceous and Paleocene Strata

The "odd conglomerate" bed of Lehman and Busbey (2007) has thus far been identified only at the Dawson Creek and Rough Run Creek exposures of the K-Pg contact interval (Fig. 2). No similar deposits have been recognized at any of the K-Pg contact exposures on the eastern side of the Park. Admittedly however, in most areas, the "odd conglomerate" is a thin, discontinuous, and obscure bed that is easily overlooked, particularly in areas where Quaternary alluvial cover is extensive. At Rough Run Amphitheater, there are two distinct beds of conglomerate separated by an interval of 20 m (Fig. 2, section #3; Fig. 6A).

The "odd conglomerate" bed is regarded as odd because in most areas it is very thin, very coarse grained, and differs in texture and composition from typical fluvial conglomerate beds (basal part of Facies 2; Fig. 2) in the underlying Javelina Formation and overlying Black Peaks Formation. Fluvial channel deposits in these strata ordinarily range from 3 to 7 m in thickness (Facies 2 in Fig. 2; Lehman, 1991; Lehman et al., 2018). In contrast, the "odd conglomerate" is generally no more than 20–50 cm thick, and only 1–2 m at its thickest points (Cobb, 2016). Typical fluvial channel deposits in the Javelina and Black Peaks formations also have only thin lenses of conglomerate at their base, usually less than 30 cm thick, and consist instead primarily of several meters of cross-bedded, parallel-laminated, and ripple cross-laminated sandstone (facies 2 in Fig. 2). The "odd conglomerate" is in contrast composed almost entirely of gravel with little or no overlying sandy channel bar deposits (upper part of Facies 2; Fig. 2). Gravel in the "odd conglomerate" is also much coarser grained, including in many places large cobbles and a few isolated boulders up to 1 m in diameter (Cobb, 2016). In contrast, gravel in the base of fluvial channel deposits elsewhere in the Javelina and Black Peaks formations is no coarser than medium pebble size (<4 cm diameter; e.g., Lehman, 1991). Reworked pedogenic carbonate nodules, abraded petrified wood, bone, and chert comprise the usual gravel clast types in typical fluvial channel deposits (Lehman, 1991). Although some of the same clasts are also found in the "odd conglomerate," it is instead composed predominantly of sandstone clasts and contains appreciable reworked charcoal (Cobb, 2016). Therefore, whatever process was responsible for deposition of the "odd conglomerate," it appears to record an unusual sedimentation event that occurred at or around the end of Cretaceous time. A similar event of its kind had apparently not occurred prior to or following it during deposition of the Tornillo Group.

Cobb (2016) suggested that the "odd conglomerate" bed could be a deposit left by run-up or recession of the hypothesized tsunami generated by the Chicxulub impact at the K-Pg boundary, based on the unusual attributes of the bed (reviewed below) and its position within the K-Pg contact interval, as well as its general similarity to conglomeratic deposits attributed to tsunami generated by the Chicxulub impact elsewhere around the Gulf of Mexico (e.g., Bourgeois et al., 1988; Stinnesbeck et al., 1993; Smit et al., 1996; Lawton et al., 2005; Schulte et al., 2010). However, the maximum depositional age estimate of ca. 63 Ma (described below) indicates that this bed was deposited ~3 million years after the K-Pg boundary impact event.

Features of the "Odd Conglomerate" Bed

The "odd conglomerate" exhibits two sedimentary facies that differ primarily in texture and structure, referred to here as Facies A and B. In most areas, the conglomerate is a very thin (10–50 cm) bed of poorly sorted, chaotically oriented, matrix-supported, pebble and/or cobble gravel with sparse "outsized" isolated boulders and a matrix of sandy mudstone (Facies A, Figs. 6 and 7). There is little or no grain-size segregation from base to top of the deposit, although in some areas, there is crude coarsening-upward grading with largest clasts at the top of the bed (Fig. 7). The gravel consists of subangular large clasts of sandstone, subrounded smaller clasts of mudstone, pedogenic carbonate nodules, bone, and charcoal.

In contrast, in a few areas, the "odd conglomerate" forms much thicker (1–2 m) lenses. In these areas, the conglomerate is well stratified and consists of moderately sorted and rounded, horizontally bedded, clast-supported, pebble and/or cobble conglomerate grading upward to parallel-laminated, coarse- or medium-grained sandstone (Facies B, Figs. 7 and 8). As many as three successive fining-upward graded beds are evident in some exposures (Fig. 8). The gravel clasts are of the same composition as in Facies A, although carbonate nodules are more abundant. Cobb (2016) found that Facies B lines the floor of a "paleo-valley" incised within the underlying Black Peaks Formation at the Rough Run East outcrop (Fig. 9). As exposed, this paleo-valley is ~800 m in width, and is filled with up to 30 m of thinly bedded carbonaceous mudstone (unit 7 of Fig. 9; Cobb, 2016) that pinches out at the margins of the paleo-valley. Facies A of the "odd conglomerate" forms a thinner mantle on the flanks of the paleo-valley and is much more extensive laterally beyond the valley-fill, resting on the correlative erosional surface in surrounding strata. At the Rough Run Amphitheater outcrop, there are two distinct beds of conglomerate (Fig. 2, section #3); the lower of these two beds is a thick lens that exhibits features of Facies B; the upper bed instead exhibits characteristics of Facies A.

All of the clasts in the conglomerate appear to be of local derivation. No extra-basinal or "exotic" clast types have been recognized. Sandstone clasts comprise the largest cobbles and boulders. Petrographic study of these indicates that they were probably derived from erosion of sandstones in the Javelina or

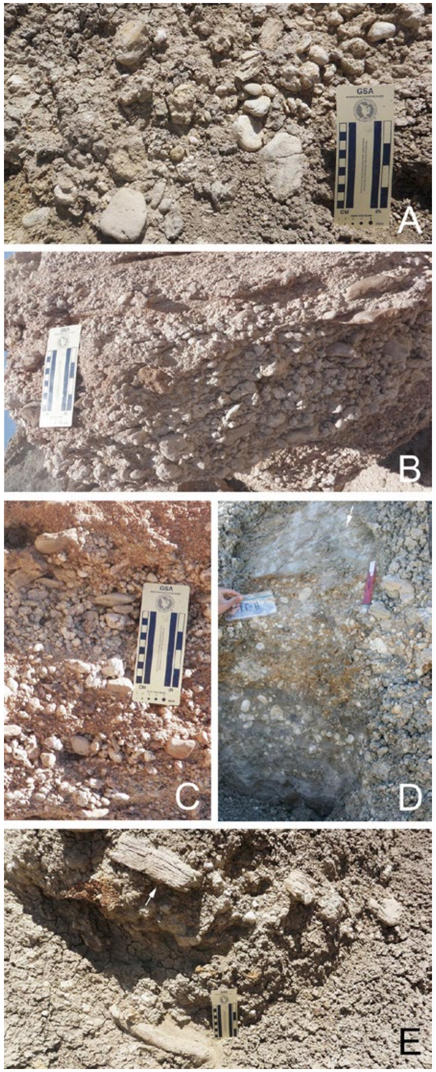

Figure 7. Photographs showing features of the "odd conglomerate" at the Rough Run Creek exposure: (A) Facies A with typical poorly stratified, poorly sorted, matrix-supported texture; (B) Facies B with finer-grained, stratified, moderately sorted, grain-supported texture; (C) Facies B with grain-supported texture and fining-upward grain-size gradation; (D) Facies A showing matrix-supported texture and lack of vertical grain-size trend or crude inverse-grading; (E) Facies A showing matrix-supported texture; arrows indicate examples of subangular outsized sandstone clasts.

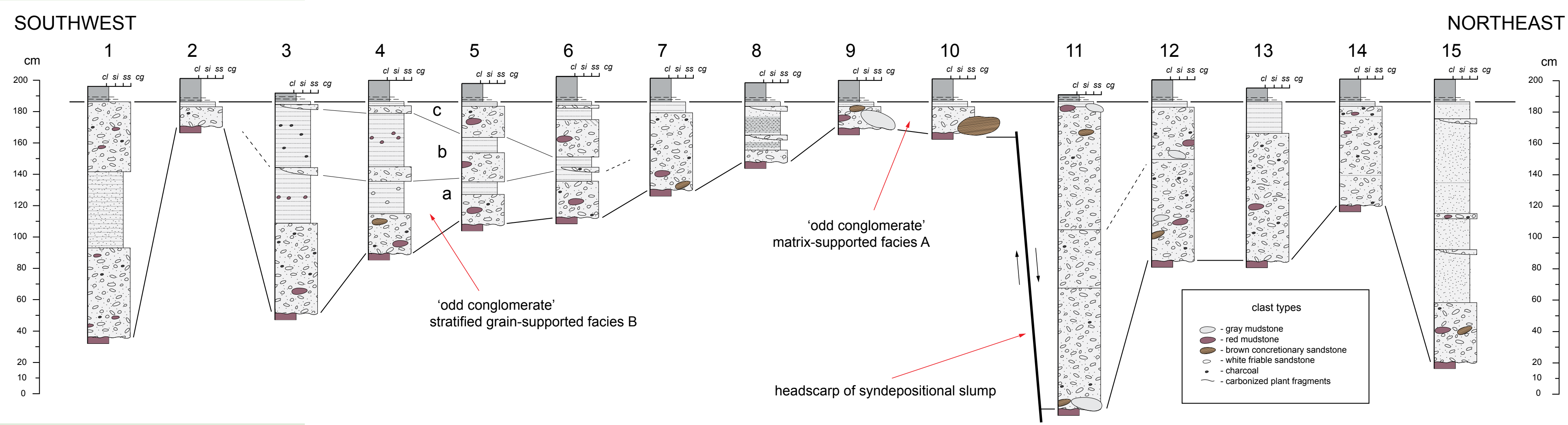

Figure 8. Correlation of detailed measured sections through the "odd conglomerate" bed at the Rough Run East exposure of the Cretaceous-Paleogene (K-Pg) contact interval (section #4 of Fig. 2; modified from Cobb, 2016) showing lateral variation in thickness between thick, finer grained, stratified, grain-supported Facies B (with multiple sedimentation units a, b, and c) and thin, coarser grained, matrix-supported Facies A. Top of "odd conglomerate" is chosen as the datum for correlation, however, both base and top of unit show substantial depositional relief (see Fig. 9).

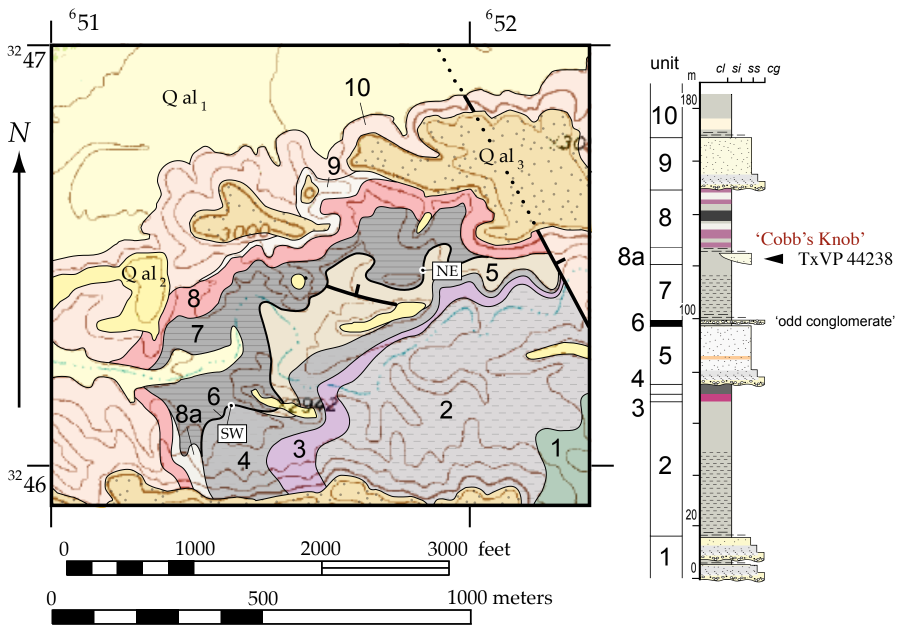

Figure 9. Detailed geologic map of the Rough Run East exposure (modified from Cobb, 2016) showing extent of numbered stratigraphic units (section #4 of Fig. 2) above and below the paleo-valley floored by "odd conglomerate" bed, and southwestern (SW) to northeastern (NE) extent of stratigraphic cross-section shown in Figure 8. Unit 7 overlying the "odd conglomerate" (unit 6) thins and pinches out at margins of paleo-valley.

Black Peaks formations, perhaps even from directly underlying sandstone beds in the immediate vicinity (Fig. 10; Cobb, 2016). Although the sandstone pebbles in the "odd conglomerate" tend to have fewer feldspar grains and more sedimentary lithic grains, they were derived from lithic to sublithic sandstones with abundant sedimentary and volcanic rock fragments such as sandstones typical of the Javelina and Black Peaks formations (Fig. 10).

The mudstone "rip-up" clasts and carbonate rock fragments were also likely derived from erosion of nearby mudstone beds with pedogenic carbonate nodules (e.g., Lehman, 1989). Although charcoal clasts occur sparingly in other Tornillo Group conglomerate beds, charcoal is a common constituent of the "odd conglomerate." The charcoal clasts are rounded and must have been transported some distance prior to deposition, although likely not far given their softness compared to other clasts. The sandstone clasts are also slightly rounded, indicating that they were similarly subject to some transport prior to deposition. However, even today (after prolonged burial diagenesis and exhumation), sandstone beds in the Black Peaks Formation are only weakly indurated with clay and calcite cement, and clasts derived from them disintegrate in modern streams a short distance from the outcrop. The sandstone beds that were the source of the clasts in the "odd conglomerate" were likely even less indurated prior to burial diagenesis, and therefore, these clasts would similarly have rounded in a short time and not survived prolonged transport. In summary, all of the clast types represented in the "odd conglomerate" appear to reflect derivation from very nearby source areas.

Vertebrate bones and teeth are rare in the "odd conglomerate," and all examples thus far observed are so fragmentary, isolated, and abraded that it seems reasonable to interpret them as having been exhumed and re-deposited from older strata (e.g., TxVP 44218-1, a broken tyrannosaurid tooth). All of the examples thus far discovered clearly pertain to dinosaurs or other large Cretaceous vertebrates, but no convincing example of a whole in situ bone has been located or collected from the "odd conglomerate."

Cobb (2016) selected sand grains from the matrix of the "odd conglomerate" and from the fine-grained layer at its top to determine if components elsewhere associated with the K-Pg impact horizon (e.g., microspherules and "shocked" quartz grains) could be identified here. Of 122 grains that he examined using SEM-EDS, four quartz grains appear to show planar deformation features, and six are siliceous spherule-like grains with "splash" or "ablated" morphologies.

Of the four quartz grains with sets of planar micro-features, three grains show multiple prominent sets of planar lamellae, and one shows sets on multiple faces (Figs. 11A–11C). The lamellae are parallel, with spacing between 5 and 20 microns, and with intersections in places showing "side-stepping" geometry (Fig. 11D). Parallel sets of micro-fractures, also with ~20 micron spacing, are present on another quartz grain; the fractures do not appear to extend across the entire grain, smaller fractures are evident between more prominent ones, and some of the fractures have splays at their ends. These four grains exhibit at least some of the features reported in quartz grains subject to "shock" metamorphism, as is typically associated with bolide impact sites and ejecta (e.g., Stöffler and Langenhorst, 1994; Mahaney, 2002).

Many grains in the sample appear in reflected light to be clear glass spheres and are found to be composed primarily of SiO_2 when examined using EDS under SEM (Figs. 11E–(11G). However, most of these grains can be arrayed along a morphological spectrum from completely anhedral spherical grains to others that exhibit rounded subhedral or

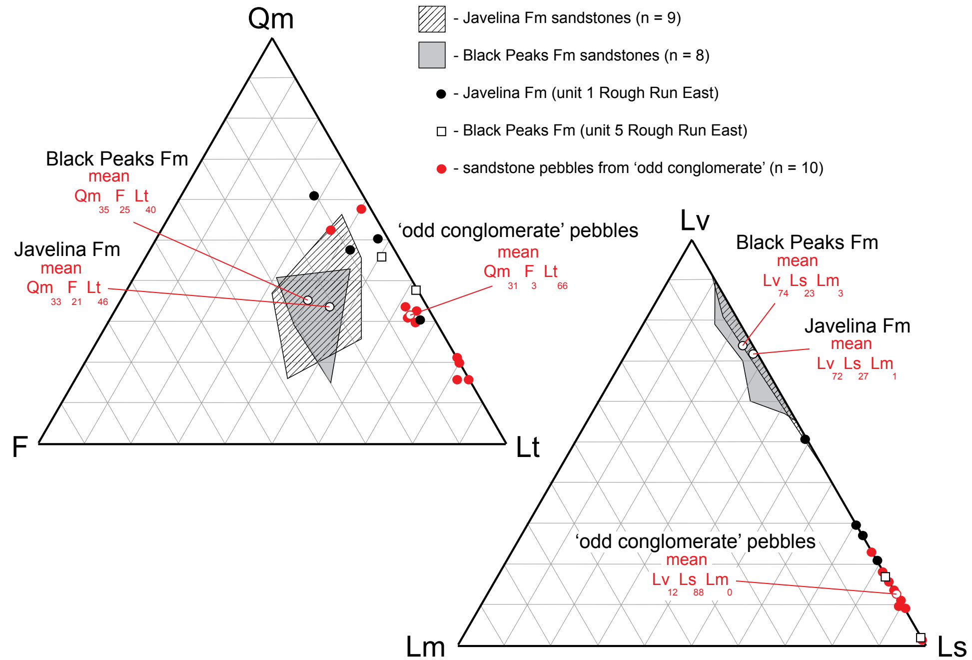

Figure 10. Mineralogical composition of sandstone clasts in the "odd conglomerate" compared with composition of sandstones in the Javelina Formation and lower Black Peaks Formation (data from Lehman, 1991) and sandstone beds exposed at the Rough Run East outcrop (data from Cobb, 2016; units 1 and 5 shown in Fig. 9); based on thin-section point counts of minimum 100 framework grains using methods given by Folk (1980); Qm—quartz (monocrystalline and polycrystalline grains); F—feldspar; Lt—total lithic grains (including chert); Lv—volcanic lithic grains; Lm—metamorphic lithic grains; Ls—sedimentary lithic grains.

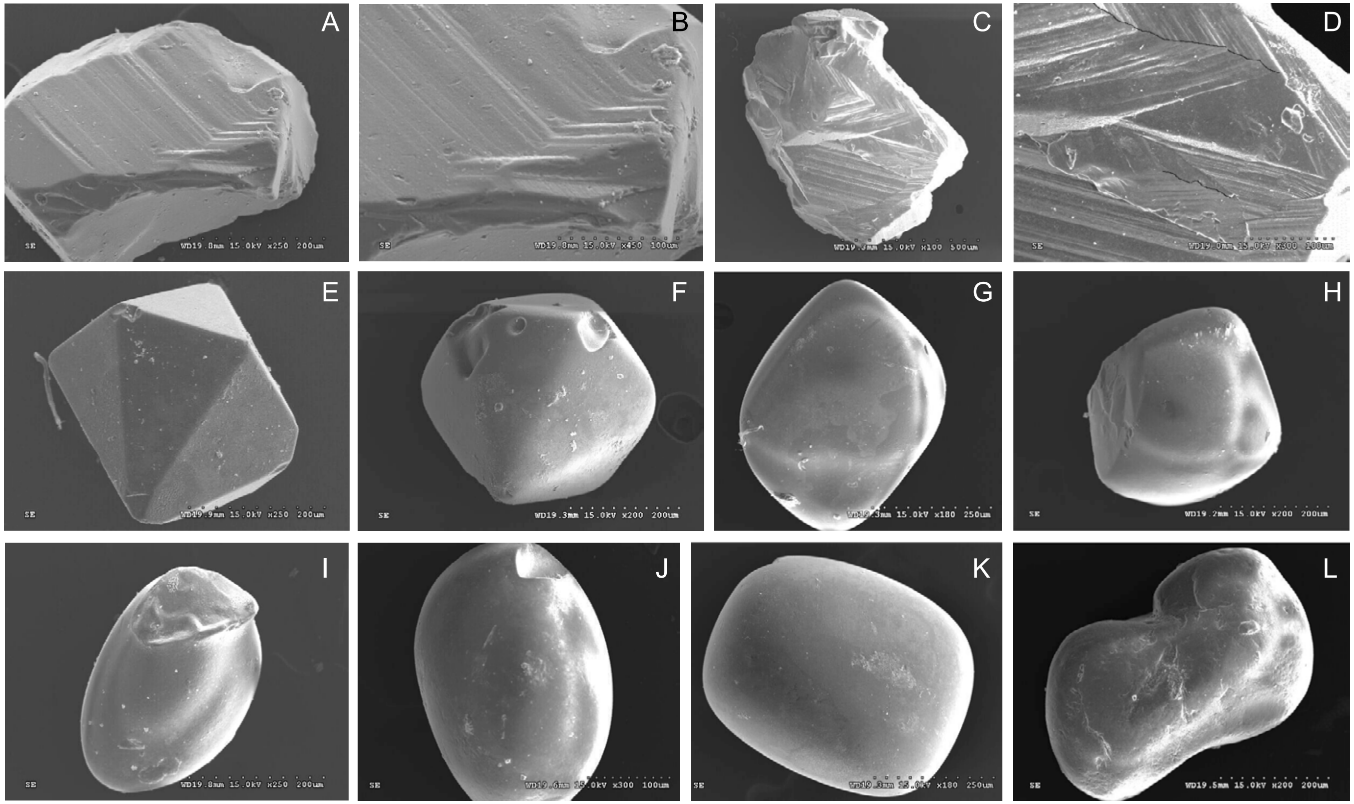

Figure 11. Scanning electron microscopy (SEM) photographs showing features of selected quartz grains separated from the "odd conglomerate" bed at the Rough Run East exposure (modified from Cobb, 2016): (A) quartz grain showing planar micro-features; (B) detail of grain shown in image A; (C) multiple intersecting sets of planar lamellae; (D) detail of grain shown in image C highlighting "side stepping" intersections of planar lamellae; (E) grain showing well-faceted euhedral hexagonal bipyramidal (β quartz) form; (F) grain with modified rounded bipyramidal form; (G) grain showing subspherical form with projecting flanges; (H) "saucer-shaped" grain with bulbous center and external flange; (I) "saucer-shaped" grain; (J) "saucer-shaped" grain; (K) oblong subspherical grain; (L) "dumbbell-shaped" grain.

faceted euhedral, hexagonal bipyramidal (β quartz) form typical of quartz phenocrysts in volcanic and shallow intrusive rocks (e.g., Smyth et al., 2008). It seems likely that most of these spherule-like grains are actually varied volcanic quartz grains modified by partial resorption (e.g., Müller et al., 2009) and derived from erosion of felsic pyroclastic deposits.

Some spherule-like grains, however, are not readily interpreted as derived through resorption or modification of hexagonal bipyramidal form. There are "saucer-shaped" grains that exhibit a thick bulbous center and a thin external flange (Figs. 11H–11K). There are also "dumbbell-shaped" grains that resemble two spheres joined together and surrounded by a thin external flange (Fig. 11L). These grains are comparable in shape to "splash form" microtektites, which are known to result from impact events (Glass, 1990). Even so, the great bulk of sand in the "odd conglomerate" exhibits features typical for detrital quartz grains; these few unusual grains are quite rare.

Charophyte Flora

Charophyte algal gyrogonites are common throughout the uppermost sandy interval of the "odd conglomerate" at the Rough Run East exposure, and at least four species are represented in this assemblage (Fig. 12; Cobb, 2016). The most abundant species is *Platychara compressa* (Peck and Reker, 1948), recognized primarily on the basis of its distinctive oblate-spheroidal shape; however, all of the specimens recovered have a slightly

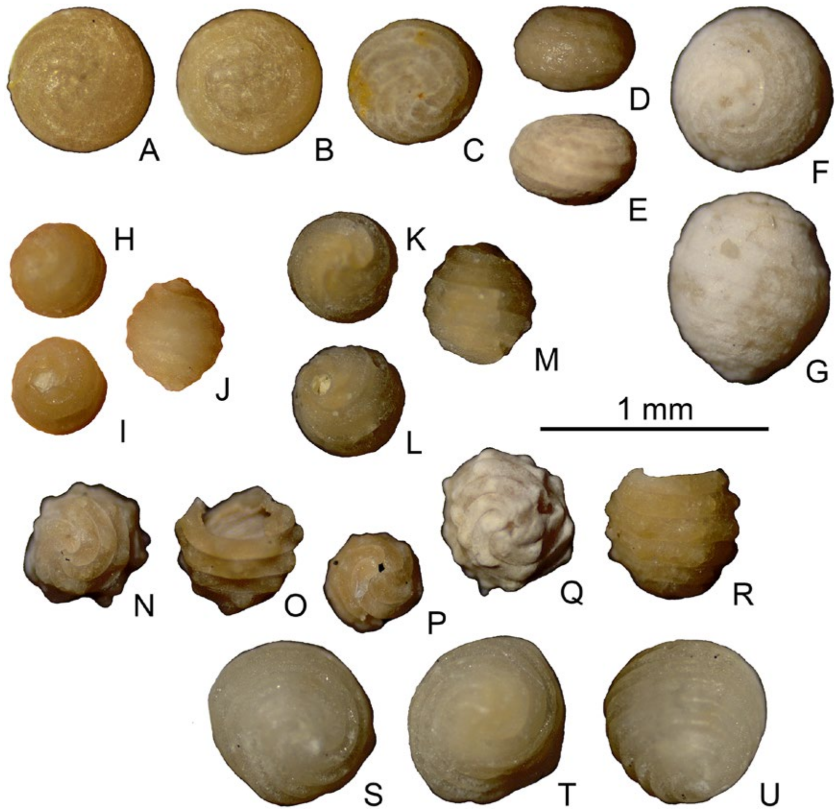

Figure 12. Examples of charophyte gyrogonites from the "odd conglomerate." ***Platychara compressa*** **(A) specimen #5 in basal and (B) apical view; (C) specimen #8 in basal view; (D) specimen #46 in lateral view; (E) specimen #1 in lateral view;** ***Porochara gildmeisteri*** **(F) specimen #31 in apical and (G) lateral view;** ***Microchara*** **cf.** ***M. leiocarpa*** **(H) specimen #43 in apical, (I) basal, and (J) lateral view; (K) specimen #12 in apical, (L) basal, and (M) lateral view;** ***Strobilochara*** **sp., (N) specimen #24 in basal, and (O) oblique lateral view; (P) specimen #60, basal view; (Q) specimen #27 in basal view; (R) specimen # 28 in lateral view; indeterminate charophyte (S) specimen #11 in basal, (T) apical, and (U) oblique lateral view.**

smaller diameter than those measured by Peck and Forester (1979). Also abundant is *Strobilochara* sp., with pronounced tuberculate ornamentation (e.g., Mebrouk et al., 2009); although all of the specimens recovered are incomplete, none preserves the apical part of the gyrogonite, and the species cannot be identified with certainty. Small specimens referred to *Microchara* cf. *M. leiocarpa* (Grambast, 1971) are also common, and these are relatively well preserved. A few specimens are referable to *Porochara gildmeisteri* (Koch and Blissenbach, 1960), and several others remain unidentified.

This charophyte assemblage is very similar to one found in the Upper Cretaceous (Maastrichtian) part of the North Horn Formation in central Utah (Fouch et al., 1987). The North Horn charophyte flora includes *Platychara compressa*, *Porochara gildmeisteri*, *Microchara* cf. *M. cristata*, *Microchara* cf. *M. leiocarpa*, *Strobilochara* n. sp., and *Retusochara* n. sp.

Platychara compressa is typical of Upper Cretaceous strata in North America, although Peck and Forester (1979) reported an occurrence also in the lower Paleocene of Alberta. *Microchara cristata* and *M. leiocarpa* are known from Maastrichtian strata of Europe (Grambast, 1971), but *Microchara* spp. extends through the Paleocene (Riveline et al., 1996). *Strobilochara* spp. are typical of Maastrichtian strata in Europe and North Africa (Mebrouk et al., 2009). *Porochara gildmeisteri* is known from Maastrichtian strata of South America (Musacchio, 2000). Taken together, the charophyte species identified suggest a Maastrichtian age for the flora found in the upper part of the "odd conglomerate."

At least two of the same charophyte taxa (*Platychara compressa* and *Porochara gildmeisteri*) also occur at the Grapevine Hills exposure, in a thin gastropod-rich limestone bed that intervenes between the highest in situ dinosaur specimen (TxVP 43621-1, juvenile *Alamosaurus sanjuanensis*; Lehman and Coulson, 2002) and the lowest Paleocene site (TxVP 44234 "Hoplochelys Ridge"; see Fig. 2). Here, and elsewhere, abundant aquatic invertebrates (gastropods, bivalves) are found in the uppermost Cretaceous strata immediately below the K-Pg contact interval, indicative of a widespread episode of freshwater subaqueous depositional conditions (e.g., Lehman, 2021).

Mammalian Fauna

Most of the Paleocene vertebrate fossil sites within the K-Pg contact interval have yielded a diverse but biostratigraphically non-diagnostic assemblage of fishes, turtles, and crocodylians. Although some of these non-mammalian taxa are typical of Paleocene faunas (e.g., the kinosternoid turtle *Hoplochelys*; but see Knauss et al., 2011), they have relatively long stratigraphic ranges and are of little use in constraining the age of these faunas. Mammalian fossils are rare and have only been recovered at eight of the sites, and of these, only the Dogie and Tom's Top sites have been subjects of screen-washing efforts. Mammalian specimens at the other six sites were obtained entirely by surface collection. Although Standhardt (1986) and Leslie et al. (2018a) provide a thorough account of mammalian taxa recovered at the Dogie (TxVP 42327) and Tom's Top (TxVP 41400) localities, we report herein a few additional species also from those localities, and we describe the mammalian specimens recovered at the other Paleocene localities known from immediately above the K-Pg contact (Table 1, Figs. 13–15). In the following descriptions for each of the mammalian taxa, the known biostratigraphic range is shown in North American Land Mammal Age (NALMA) interval zones, as given by Williamson (1996), Archibald (1998), and Lofgren et al. (2004). Where sources differ, the longer range is shown.

Abbreviations: H—height, L—length, W—width, n—number of specimens measured, AW—anterior (trigonid) width, PW—posterior (talonid) width, *—an estimate based on incomplete specimen or photograph. All measurements are given in millimeters.

Order Multituberculata Cope, 1884
Family Ptilodontidae Cope, 1887
Ptilodus mediaevus Cope, 1881
Range: Puercan (Pu2) through Tiffanian (?Ti5)

TxVP 41400-28 (Tom's Top locality) is a large complete left p4 with long anterior edge, 12 serrations on the labial side, and 11 on the lingual side (Fig. 13A). In size (L = 7.7, W = 2.8, H = 7.1), labial profile, and serration count, this specimen is comparable to those assigned to *P. mediaevus* by Simpson (1937; mean L = 8.3, n = 6) and Rigby (1980; L = 6.6–9.0, mean = 8.1, n = 54).

TxVP 41400-33 (Tom's Top locality) is a right p4 missing part of the posterior edge, but of nearly identical size and form as TxVP 41400-28, and also referred herein to *P. mediaevus*. Schiebout (1974) assigned several similar specimens from higher in the Black Peaks ("T2" = TxVP 40147) also to *P. mediaevus* (see discussion by Standhardt, 1986). *Ptilodus* specimens from the Dogie locality were regarded by Standhardt (1986) as differing sufficiently from *P. mediaevus* to recognize as a new species; however, the present specimens are within the range in size and labial profile for assignment to *P. mediaevus*.

Order Taeniodonta Cope, 1876
Family Stylinodontidae Marsh, 1876
Psittacotherium multifragum Cope, 1882
Range: Torrejonian (To2) through Tiffanian (?Ti5)

TxVP 44238-1 (Cobb's Knob locality) is a worn right P1 or P2 (L = 6.2, W = 14); it is double-rooted with smooth enamel extending farther lingually than labially, bicuspid with a tall paracone, smaller protocone, little or no metacone, and a weak posterior cingulum (Figs. 13B–13C). Although TxVP 44238-1 is narrow as is P1 in *P. multifragum*, it is closer in size to P2 (e.g., mean L = 9.6, W = 15.3, n = 7; Schoch, 1986) and also double-rooted, while P1 has a single root. A specimen from higher in the Black Peaks Formation that Schiebout (1974) identified as P2 and attributed to either *Psittacotherium* or *Lampadophorous* (TxVP 40536-119; L = 9.5, W = 13.4) is also significantly wider than the present specimen.

TxVP 42327-5 (Dogie locality) is a left ?p1 (L = 6.8, W = 11.9) with a single root and smooth enamel that extends much farther aborally on the labial side (Figs. 13D–13F). The crown is simple and bicuspid with a large, slightly worn labial paracone, and a much smaller unworn lingual protocone. There is a minutely cuspidate crest linking the two cusps along the posterior base of the crown. The lower premolars in *P. multifragum* are not very well known. There are no published descriptions of p1, although its alveolus indicates that it is much smaller than p2 (e.g., Taylor, 1984). The present specimen is significantly smaller than known examples of p2 (mean L = 8.8, W = 14.4, n = 3; Schoch, 1986).

TxVP 42327-13 (Dogie locality) is a worn right m2 (L = 9.5, AW = 10.2, PW = 8.5*) with slightly crenulated enamel, and the posterior and lingual edge partly broken (Figs. 13G–13I). This is a double-rooted, transversely bilophodont tooth with a wide trigonid, and a much lower, narrower, and shorter talonid that is inset along its labial margin. The talonid basin is very narrow but deep, and open lingually. Although worn, the protoconid and metaconid are of comparable size and height; the hypoconid is the largest and only prominent cusp on the talonid. The m2 in *P. multifragum* is only known in a few other specimens (n = 3, mean L = 9.2, AW = 9.2; Schoch, 1986) but TxVP 42327-13 is closely comparable in form and size.

TxVP 42327-14 (Dogie locality) is a large taeniodont ungual "claw" also likely referable to *P. multifragum*. TxVP 40151-9 ("T10" = Robber's Roost locality) is an incisor fragment that also probably pertains to *P. multifragum*. Although Wilson (in Maxwell et al., 1967) previously reported *P. multifragum* on the basis of an associated incisor fragment, canine, and ?P3 (TxVP 40147-3) from the "T2" locality, Schiebout (1974) considered this specimen insufficient to adequately distinguish from *Lampadophorous*.

TABLE 1. MAMMALIAN TAXA REPORTED IN THIS STUDY

Taxon	Locality							
	40151	40181	41400	42327	43380	43455	44234	44238
Ptilodus mediaevus			X					
Psittacotherium multifragum	?			X				X
Chriacus baldwini				X				
Chriacus cf. *C. pelvidens*			X	X				
Deuterogonodon noletil	X							
Mimotricentes sp.				X				X
Periptychus carinidens					X	X	X	
Mioclaenus turgidus			X	X				
Mioclaenus sp.			X					
Protoselene cf. *P. griphus*					X			
Tetraclaenodon puercensis			X	X				
Phenacodus cf. *P. grangeri*		X						

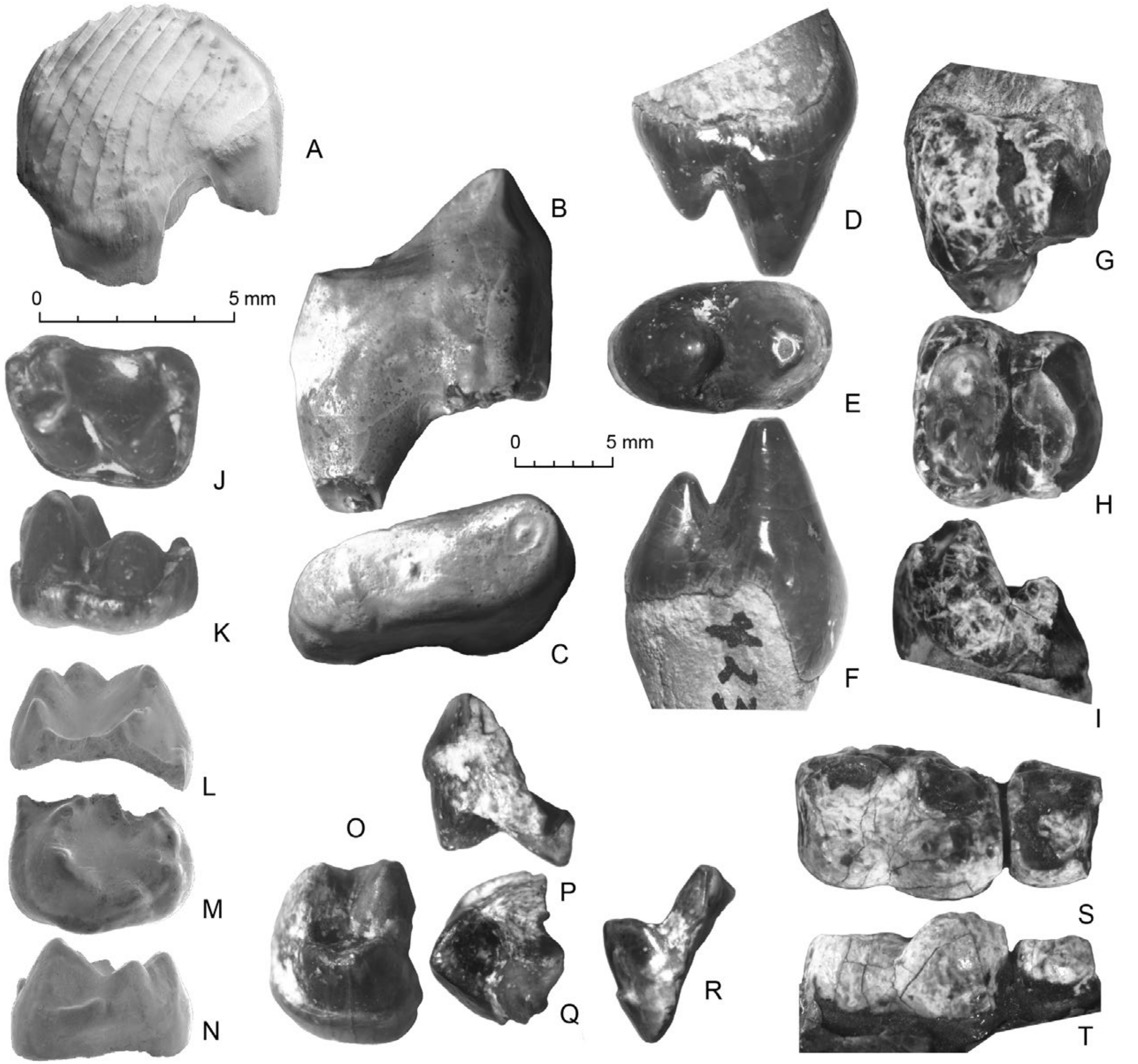

Figure 13. Selected mammal teeth from Torrejonian localities in the Black Peaks Formation. *Ptilodus mediaevus* (TxVP 41400-28) left p4 in (A) labial view; *Psittacotherium multifragum* (TxVP 44238-1) right P2 in (B) posterior and (C) occlusal view; (TxVP 42327-5) left ?p1 in (D) anterior, (E) occlusal, and (F) posterior views; (TxVP 42327-13) right m2 in (G) labial, (H) occlusal, and (I) lingual views; *Chriacus baldwini* (TxVP 42327-11) left m1 in (J) occlusal and (K) labial views; *Chriacus* cf. *C. pelvidens* (TxVP 41400-31) talonid of left ?m2 in (L) oblique anterior, (M) occlusal, and (N) posterior views; (TxVP 42327-16) trigonid of right ?m1 in (O) oblique anterior, (P) labial, (Q) occlusal, and (R) lingual views; *Deuterogonodon noletil* (TxVP 40151-1) left m2 and talonid of m1 in (S) occlusal and (T) lingual views. Large 5 mm scale bar applies to images A and J–R; small 5 mm scale applies to all remaining images.

Order Condylarthra Cope, 1881
Family Arctocyonidae Giebel, 1855
Chriacus baldwini (Cope, 1882)
Range: Torrejonian (To1) through Tiffanian (Ti4)

TxVP 42327-11 (Dogie locality) is an unworn left m1 (L = 4.9, W = 3.6) with smooth to slightly wrinkled enamel, a nearly flat lingual margin, and sharp conical cusps with flat internal surfaces. The trigonid is substantially taller than the talonid. The trigonid basin is small, deep, and enclosed, the protoconid slightly taller than metaconid, paraconid small and directly anterior to the metaconid, and all connected by cristids (Figs. 13J and 13K). There is a small cuspule on the paracristid. The talonid is long and wide, the hypoconid much larger than the entoconid, small hypoconulid close to the entoconid, and all talonid cusps connected by cristids. There are no cuspules on the entocristid, and the talonid notch is relatively open along the lingual margin. The precingulum and labial cingulum are contiguous and well developed, extending from the anterior base of the protoconid along the labial margin and ascending the posterior side of hypoconulid.

The present specimen is similar in morphology, but slightly larger than an m1 described by Schiebout (1974; TxVP 40537-88 referred to *Tricentes truncatus* [= *C. baldwini*] L = 4.6, W = 3.1), although it is slightly smaller than two also from higher in the Black Peaks (TxVP 41365; L = 5.2–5.3, W = 3.2–3.6), and one described by Taylor (1984; L = 5.5, W = 3.5) from the Nacimiento Formation.

Chriacus cf. *C. pelvidens* (Cope, 1881)
Range: Torrejonian (To2) through Tiffanian (Ti4)

TxVP 41400-31 (Tom's Top locality) is the unworn talonid of a left lower molar, probably m2 (Figs. 13L–13N). The talonid basin is deep, circular, and closed lingually. The hypoconid is larger and taller than the entoconid, and the hypoconulid is lingual to the midline. The entocristid is cuspidate, and there is a distinct entoconulid, as well as a small accessory cusp on the cristid obliqua. There is no lingual cingulid, but a labial cingulid extends to the base of the hypoconid, and there is a separate short postcingulid labial of the hypoconulid. This specimen is much larger (PW = 5.1) and more cuspidate than TxVP 41365-616 (PW = 3.6; m2 referred to *Tricentes truncatus* [= *C. baldwini*] by Schiebout, 1974), and is also beyond the upper end of the size reported for m2 in *C. baldwini* by Taylor (1984; PW = 4.1–4.7, n = 4). However, TxVP 41400-31 is well within the size range that Taylor (1984; PW = 4.4–5.4, n = 6) and Rigby (1980; PW = 4.5–5.7, n = 15) reported for m2 in *C. pelvidens*, and is referred herein to *Chriacus* cf. *C. pelvidens*.

TxVP 42327-16 (Dogie locality) is the trigonid of a right ?m1 (AW = 3.6), unworn, with smooth enamel referred here tentatively also to *C. pelvidens* (Figs. 13O–13R). The cusps are tall and conical, with sharp apices. The protoconid is slightly shorter and more anterior than the metaconid; the paraconid is well separated from the metaconid and slightly lingual to it. The trigonid notch is deep and wide. The paracristid is narrow and blade-like, as is the premetacristid, and together enclose a deep trigonid basin. The precingulid is short and restricted to the anterolabial margin. TxVP 42327-16 is within the reported size range for m1 in *C. pelvidens* (e.g., AW = 3.4–4.2, n = 2; Taylor, 1984).

Deuterogonodon noletil Van Valen, 1978
Range: Torrejonian (To1 through To2)

TxVP 40151-1 ("T-10" Robber's Roost locality) is a left mandible fragment preserving m2 and the talonid of m1 (Figs. 13S and 13T). The m2 (L = 10.1) has trigonid slightly higher than the talonid and of comparable width. Although the labial edge is damaged, the metaconid is slightly smaller but comparable in height to the protoconid, and slightly posterior to it. There is a small but distinct conical paraconid separated from and directly anterior to the metaconid. The talonid basin is open lingually, with high hypoconid linked to smaller hypoconulid and entoconid, and all cusps linked by cristids. The m2 is smaller than that in *D. montanus* (L = 12.6; Simpson, 1937) but comparable in size to that in *D. noletil* (Taylor, 1984; L = 9.3).

Wilson (in Maxwell et al., 1967) originally referred this specimen to ?*Claenodon* cf. *C. procyonoides*, but Schiebout (1974) subsequently recognized it instead as pertaining to ?*Deuterogonodon* sp. Taylor (1984) suggested that the specimen could represent *D. noletil*, and that assignment is supported here.

Mimotricentes sp.
Range: Torrejonian (To1) through Tiffanian (Ti6)

TxVP 42327-15 (Dogie locality) is a nearly unworn left M3 (L = 5.1, W = 7.0) with crenulated enamel and pustulate trigon basin (Figs. 15A–15C). A prominent cingulum almost completely encircles the tooth, but does not quite pass the base of the paracone, and merges with the posterior side of the metaconule. The crown is nearly oval in occlusal view, with no ectoflexus. Both paracone and protocone are blunt, conical, and comparable in height, but the metacone is highly reduced and closely appressed to the posterolingual side of the paracone. The paraconule is prominent and nearly as large as the metacone. The metaconule is low; the postprotocrista is well developed and extends to the postcingulum.

The crenulated enamel, encircling cingulum, nearly oval crown with low cusps, and highly reduced metacone are much like that in *Mimotricentes subtrigonus*. However, the present specimen is slightly larger than the M3 specimens of *M. subtrigonus* measured by Taylor (1984; W = 6.1–6.7, n = 4) and also larger than any in the large sample studied by Rigby (1980; W = 5.4–6.75, n = 52).

TxVP 44238-2 (Cobb's Knob locality) is a slightly worn right m3 (L = 7.4, AW = 5.4) with blunt conical cusps, crenulated enamel, and talonid basin also crenulated (Figs. 15D–15F). The crown is relatively wide and quadrangular, with talonid only slightly narrower than trigonid. The metaconid is slightly taller than the protoconid, and the two are closely situated. A continuous paracristid extends to the weak paraconid anterior and medial to the metaconid. The precingulum is contiguous with the lingual cingulum. Talonid cusps are of comparable height, with the hypoconulid slightly taller than hypoconid and entoconid. There is a short postcingulid on the lingual side of the hypoconulid.

The highly crenulated enamel, low cusps with trigonid and talonid of comparable height, weak paraconid central on the paracristid, and lingually projecting entoconid are all like that in *Mimotricentes subtrigonus*. However, this specimen is larger than those from the Nacimiento Formation measured by Taylor (1984; L = 6.1–6.9, n = 12) or any in the large sample from the Fort Union Formation measured by Rigby (1980; L = 5.7–7.2, n = 75).

Both TxVP 44238-2 and 42327-15 appear to pertain to the same taxon, similar to *Mimotricentes subtrigonus*, but both are slightly larger than other reported specimens. They are referred herein to *Mimotricentes* sp.

Family Periptychidae Cope, 1881
Periptychus carinidens Cope, 1881
Range: Torrejonian (To1) through Tiffanian (Ti4)

TxVP 43380-1 (Yellow Hill locality; see Straight, 1996) is a partial right maxilla with slightly worn P4 to M2 (Figs. 14A–14B). Lengths and widths (in mm) are for P4 (13.3 and 13.9), P5 (11.9 and 15.1), M1 (11.1 and 13.8), and M2 (10.9 and 13.3), respectively. All teeth have strongly corrugated enamel with ribs radiating from the crowns on both lingual and labial sides, and shallow (not expanded) lingual slopes. The premolars have tall, inflated paracones, slightly inclined posteriorly, with small parastyle and metastyle. The protocone on premolars have a marked series of cuspules that form a crescentic lingual shoulder. P5 is shorter and wider than P4, and has a more pronounced lingual lobe, skewed anteriorly. The molars are nearly quadrangular in occlusal view, with conical paracone and metacone of comparable size, weak centrocrista, and weak parastyle but with metastyle forming a distinct small cusp. The protocone is low, with well-developed pre- and postprotocrista. Paraconule and metaconule are small and of comparable size. The hypocone is large, and on M2 extends lingually farther than the protocone. There is a small cuspule posterior and labial of the hypocone on M2. Pre- and postcingulum are well developed, but ectocingulum is very weak.

In size and morphology, the teeth in this specimen are compatible with the revised diagnosis for *P. carinidens* given by Shelley et al. (2018). The present specimen is slightly larger than others (TxVP 40147-4 and -17) from the Black Peaks referred to as *P. carinidens* by Wilson (in Maxwell et al., 1967); however, Taylor (1984) noted that Wilson's specimens are also smaller than those pertaining to *P. carinidens* from the Nacimiento Formation (for M1 L = 8.8–13.8, mean = 9.7, W = 10.7–12.3, mean = 11.5; for M2 L = 8.9–10.3, mean = 9.4, W = 10.4–11.8, mean = 11.1; n = 5). In contrast, the present specimen is significantly smaller than others (TxVP 40537-59) that Wilson (in Maxwell et al., 1967) and Schiebout (1974) referred instead to *P. superstes*. Although Williamson (1996) and Shelley et al. (2018) subsequently considered *P. superstes* a junior synonym of *P. carinidens*, they also noted that some of the Black Peaks specimens fall outside the size range of those otherwise referred to *P. carinidens*.

TxVP 44234-1 (Hoplochelys Ridge locality) is a slightly worn right m2 (Figs. 14C–14E). The crown (L = 9.9, AW = 9.4, PW = 9.3) has strongly corrugated enamel, with trigonid wider and longer than the talonid. The protoconid is slightly taller than metaconid and linked by a strong protocristid; the paraconid is anterior to metaconid, and the postmetacristid is strong, spanning the talonid notch. Entoconid and hypoconid are conical and of comparable height; the hypoconulid is small and closer to the hypoconid. There is a small accessory cusp on the cristid obliqua. There is a weak lingual cingulum and postcingulum. The specimen agrees in size and morphology with m2 in *Periptychus carinidens* (e.g., Taylor, 1984; L = 8.7–10.8, mean = 9.76; AW = 7.2–10.0, mean = 8.4; PW = 6.7–9.7, mean = 8.5; n = 5) and is substantially smaller than specimens assigned to *P. superstes* by Schiebout (1974) from higher in the Black Peaks (e.g., TxVP 40537-59; L = 13.2).

TxVP 43455-1 (Periptychus locality) is a fragmentary right P5 missing the entire lingual shoulder (Figs. 14F–14G). It is smaller (L = 10.4 mm) than in TxVP 43380-1. The enamel is strongly corrugated with ribs radiating from the crown. The paracone is tall and inflated, only slightly inclined posteriorly, with small parastyle and metastyle. The protocone is broken off.

This specimen is also at the low end of the typical size range for P5 in *P. carinidens* (e.g., L = 10.6–12.4, mean = 11.2; Taylor, 1984, Ojo Encino sample). Although smaller, the specimen compares well in form with P5 in TxVP 43380-1.

Family Mioclaenidae Osborn and Earle, 1895
Mioclaenus turgidus Cope, 1881
Range: Torrejonian (To1 through To3)

TxVP 41400-29 (Tom's Top locality) is a thoroughly worn right M1 (Figs. 14K–14N). The crown (L = 5.9, W = 8.4) has smooth to slightly crenulated enamel; protocone, metaconule, and paraconule are completely worn down to the trigon basin. There is a pronounced ectoflexus, and the metacone is slightly more lingual than the paracone. The labial cingulum is continuous and well developed, and the precingulum extends from the base of the protocone to the parastyle, which forms a low round cusp.

The present specimen is at the upper end of the size range for M1 in *M. turgidus*. Taylor (1984) listed ten specimens (L = 5.0–6.1, W = 7.2–8.1) and Matthew (1937) listed seven specimens (L = 5.5–6.5, W = 6.6–8.6), all from the Nacimiento Formation, and of these, only two are as large as TxVP 41400-29. All of these, as well as the present specimen, are substantially larger than an M1 from the Dogie locality (LSU V-891; L = 4.6, W = 5.9) referred to a new species of *Mioclaenus* by Leslie et al. (2018a; see also Standhardt, 1986).

TxVP 42327-12 (Dogie locality) is the posterior end of a right mandible with deeply worn m1, m2, and m3 (Figs. 14H–14J). A few associated fragments of mandible with roots of the premolars cannot be confidently reunited with the rest of the specimen. All of the molars are large, with bulbous crowns and smooth enamel; lengths and widths (in mm) are for m1 (7.4 and 6.5), m2 (7.5 and 7.0), and m3 (7.0 and 5.5), respectively. The crown in m1 is rectangular, with trigonid and talonid of comparable size, but the entire occlusal surface is worn, and the form of cusps is no longer evident. The crown in m2 is larger and of similar rectangular form, but with the anterolingual side enlarged. It is not quite so worn; a remnant of the talonid notch suggests that the hypoconid was large. The m3 is smaller and narrower; the protoconid is large, paraconid small and directly appressed to the anterior side of the metaconid. The talonid notch is deep, and the hypoconid is large, but the posterior cristid is deeply worn, and the form of other talonid cusps is uncertain.

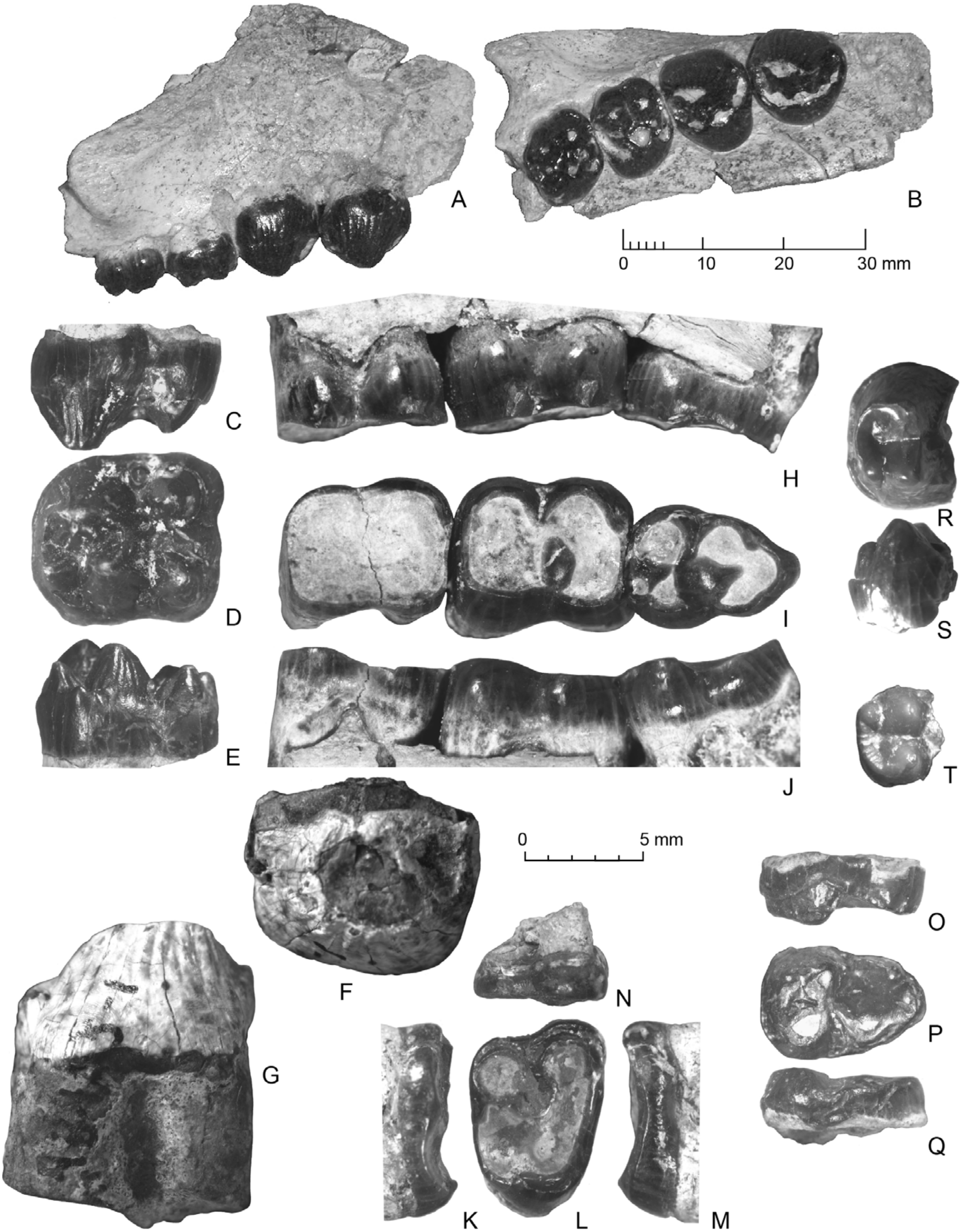

Figure 14. Selected mammal teeth from Torrejonian localities in the Black Peaks Formation. *Periptychus carinidens* (TxVP 43380-1) partial right maxilla with P4 to M2 in (A) labial and (B) occlusal views; (TxVP 44234-1) right m2 in (C) labial, (D) occlusal, and (E) lingual views; (TxVP 43455-1) labial half of right P5 in (F) occlusal and (G) labial views; *Mioclaenus turgidus* (TxVP 42327-12) posterior end of right mandible with m1, m2, and m3 in (H) labial, (I) occlusal, and (J) lingual views; (TxVP 41400-29) right M1 in (K) posterior, (L) occlusal, (M) anterior, and (N) labial view; (TxVP 42327-10) left m3 in (O) lingual (P) occlusal, and (Q) labial view; (TxVP 41400-35) right ?m2 trigonid in (R) occlusal and (S) lingual view; *Mioclaenus* sp. (TxVP 41400-32) trigonid of left lower molar (?m3) in (T) occlusal view. Lower molars are shown with anterior side to left, upper molars are shown with labial side toward top of page; 30 mm scale bar applies to images A and B; 5 mm scale bar applies to images C–T.

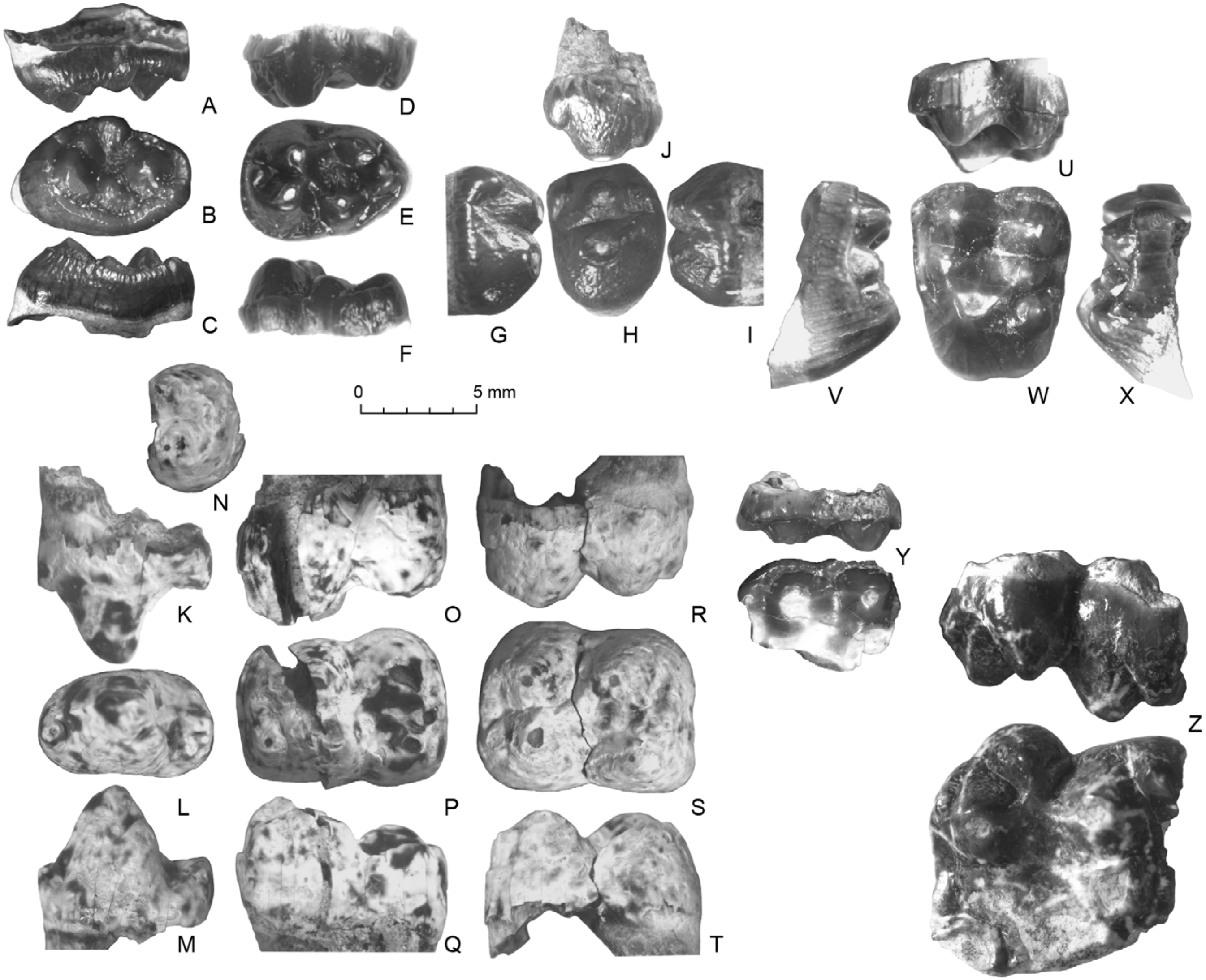

Figure 15. Selected mammal teeth from Torrejonian localities in the Black Peaks Formation. *Mimotricentes* sp. (TxVP 42327-15) left M3 in (A) anterior, (B) occlusal, and (C) posterior view; (TxVP 44238-2) right m3 in (D) labial, (E) occlusal, and (F) lingual view; *Protoselene* cf. *P. griphus* (TxVP 43380-2) right P4 in (G) posterior, (H) occlusal, (I) anterior, and (J) labial view; *Tetraclaenodon puercensis* (TxVP 42327-9) four associated teeth including right p3 in (K) labial, (L) occlusal, and (M) lingual view; heel of p4 in (N) occlusal view; right m1 in (O) labial, (P) occlusal, and (Q) lingual view; and right m2 in (R) labial, (S) occlusal, and (T) lingual view; (TxVP 41400-34) left M2 in (U) labial, (V) anterior, (W) occlusal, and (X) posterior view; (TxVP 41400-30) labial fragment of left M1 in (Y) occlusal and (above) labial views; *Phenacodus* cf. *P. grangeri* (TXVP 40181-1) fragment of right M2 in Z labial (above) and occlusal view. All lower molars are shown with anterior side to left; upper molars are shown with labial side toward top of page; 5 mm scale bar applies to all images.

The size of these molars is at the upper limit of the distribution for *M. turgidus* from the Nacimiento Formation reported by Taylor (1984; lengths for m1 = 6.1–6.9, m2 = 6.8–7.6, m3 = 5.7–7.1, n = 7), and Matthew (1937; lengths for m1 = 6.1–6.9, m2 = 6.1–6.9, m3 = 5.7–6.7, n = 6), and all of these as well as the present specimen are substantially larger than in the new species of *Mioclaenus* recognized by Leslie et al. (2018a) also from the Dogie locality (see also Standhardt, 1986).

TxVP 42327-10 (Dogie locality) is a worn left m3 (Figs. 14O–14Q) with smooth to slightly wrinkled enamel, and short stout cusps. It is very similar in form and size to the m3 in TxVP 42327-12 (described above) but not as deeply worn. The protoconid is large, paraconid is small and directly anterior to the metaconid. The talonid notch is deep, and the talonid basin is broad and shallow; the hypoconid is large, but there is no entoconid, and only a very weak hypoconulid; instead there are three minute cuspules along the posterior cristid. There is a strong precingulid and short labial cingulid. The size of this specimen (L = 6.9, AW = 4.8, PW = 3.9) is also at the upper end of the distribution for *M. turgidus* from the Nacimiento Formation reported by Taylor (1984; L = 5.7–7.1, AW = 4.4–4.8, PW = 3.5–4.0, n = 10) and Matthew (1937; L = 5.7–6.7, AW = 4.2–4.7, n = 5), and much larger than the m3 in the new species of *Mioclaenus* recognized by Leslie et al. (2018a) also from the Dogie locality (LSU V-881; for m3 L = 5.2, AW = 3.4; see Standhardt, 1986).

TxVP 41400-35 (Tom's Top locality) is the trigonid of a right ?m2 (AW = 6.5), unworn, with faintly wrinkled enamel referred here tentatively also to *M. turgidus* (Figs. 14R and 14S). The cusps are blunt and conical, with metaconid slightly taller than protoconid, paraconid only slightly shorter, and directly anterior to the metaconid from which it is separated by a narrow cleft. The paracristid is sharp, smooth, contiguous with the protoconid, and completely encircles the trigonid basin. There is a short metastylid. The precingulid extends completely around the anterior margin of the crown from the base of the paraconid to the base of the protoconid, and bears several small cuspules anterior to the paraconid. The crown is markedly constricted at the talonid notch. As with the specimens described above, TxVP 41400-35 is at the upper end of the reported size range for m2 in *M. turgidus* (e.g., AW = 6.0–6.6, n = 7; Taylor, 1984) and exceeds the sizes given for the other lower molars. Hence, if the referral to *M. turgidus* is correct, this specimen likely represents an m2.

Mioclaenus sp.
Range: Torrejonian (To1 through To3)

TxVP 41400-32 (Tom's Top locality) is the trigonid of a left lower molar (?m3; AW = 4.2) with slightly wrinkled enamel, protoconid and metaconid separate, blunt, conical, similar in height, and opposite one another, a large paraconid, distinct and directly anterior to the metaconid, and a strong paracristid extending entirely across the anterior end of the trigonid basin to the protoconid (Fig. 14T). The paracristid is crenulated with distinct cuspules on the anterolabial side of the paraconid and anterior base of the protoconid. Although this specimen has a more markedly cuspate paracristid, it is similar in morphology, and only slightly larger than the m3 in the new species of *Mioclaenus* recognized by Leslie et al. (2018a) from the Dogie locality (LSU V-881; AW = 3.4; see Standhardt, 1986). The present specimen may record this species also at the Tom's Top locality.

Protoselene cf. *P. griphus* (Gazin, 1939)
Range: Torrejonian (To1)

TxVP 43380-2 (Yellow Hill locality; Straight, 1996) is a right P4 (L = 6.2, W = 5.0), oval in occlusal view, with a stout blunt crown, wrinkled and crenulated enamel, a bifurcated labial root, and single lingual root (Figs. 15G–15J). The prominent conical paracone and protocone are of comparable height; the metacone is much smaller. There are a small parastyle and metastyle and a weak precingulum and postcingulum.

This specimen is nearly oval in occlusal view, and has slightly weaker metastyle and parastyle, but is otherwise similar in form to P4 in *P. griphus*. It is quite a bit smaller than in the type specimen (= *'Dracoclaenus' griphus* of Gazin, 1939; L = 8.3*, W = 5.7*) but about the same size as a referred specimen shown by Williamson and Lucas (1992; L = 6.3*, W = 5.2*). Very few specimens of *P. griphus* are known; so slight variations such as in the present specimen are of uncertain significance. We refer the specimen here to *Protoselene* cf. *P. griphus*.

Family Phenacodontidae Cope, 1881
Tetraclaenodon puercensis Cope, 1881
Range: Torrejonian (To1) through Tiffanian (Ti1)

TxVP 42327-9 (Dogie locality) comprises four associated teeth that were recovered in series adjacent to one another, and certainly pertain to a single individual; these are a right p3, heel of p4, m1, and m2 (Figs. 15K–15T). The crowns are poorly preserved (m1 is fractured through the trigonid), but the morphology is clear, and the stout bunodont cusps are only slightly worn. The p3 (L = 7.3, W = 4.5) has a distinct precristid and small paraconid anterior and lingual to the tall protoconid, and a basined heel with several weak cusplets along the posterior rim. Only the talonid heel of p4 is preserved (W = 5.3); it is bicuspid with a strong entoconid and hypoconid; the hypoconulid is very weak. The trigonid and talonid in both m1 (L = 8.6* AW = 6.6, PW = 6.8) and m2 (L = 9.5, AW = 7.3, PW = 7.0) are nearly the same height, with metaconid slightly taller than protoconid. Both molars have strong paracristids, but only m1 has a distinct paraconid. Both have small hypoconulids. Precingulum and postcingulum are present, but better developed on m1 than on m2.

These teeth agree in morphology with those of *T. puercensis* and are at the upper end of the size distribution reported by West (1976) for the Rock Bench locality (m2 L = 7.1–8.5, mean = 8.0, n = 17), and by Taylor (1984) for the lower Nacimiento Formation (m2 L = 7.8–9.5, mean = 8.8, n = 28), but well within the size range Taylor reported for the upper Nacimiento (m2 L = 8.1–10.0, mean = 9.1, n = 7).

TxVP 41400-34 (Tom's Top locality) is a left M2 (L = 6.6, W = 8.4), complete and only slightly worn, with slightly corrugated enamel, particularly on the labial side of the crown and on the anterior face of the protocone (Figs. 15U–15X). The crown is rectangular, and the cusps are blunt and round, except for the protocone, which is crescentic with distinct pre- and postprotocristae. The paracone and metacone are connected by a distinct centrocrista, but paracrista and metacrista are weak. Paraconule and metaconule are large and distinct, as is the hypocone, which is independent and slightly labial to the protocone. The parastyle is small but distinct. There is no metastyle or mesostyle, but the labial cingulum is minutely cuspidate. The cingulum is broad and almost completely encircles the crown labially from the anterior base of the protocone around to the posterior base of the hypocone. The metacone is slightly more lingual than the paracone, and the posterior part of the crown has slightly less labial extension; hence, TxVP 41400-34 is identified as an M2 (e.g., Taylor, 1984).

TxVP 41400-34 is substantially smaller, but very similar in form to TxVP 40147-19, an M2 (L = 8.4, W = 10.3) from the "T2" locality that Wilson (in Maxwell et al., 1967) and Standhardt (1986) assigned to *Tetraclaenodon puercensis*, but that Schiebout (1974) instead referred to *Phenacodus matthewi*. TxVP 41400-34 is certainly smaller than most upper molars referred to *Tetraclaenodon puercensis* (e.g., Taylor, 1984; Thewissen, 1990); however, both West (1976) and Williamson (1996) discussed a group of similarly small specimens, and suggested that these might represent a small subspecies, *T. puercensis 'pliciferus*,' rather than the larger and more widespread *T. puercensis 'puercensis.'* The dimensions of TxVP 41400-34 are within the size limits of this smaller population (e.g., West, 1976, Nacimiento Formation "lower Torrejon" sample M2 L = 6.2 – 8.8, n = 23).

TxVP 41400-30 (Tom's Top locality) is a broken left M1 preserving only the labial half of the crown, tentatively here also referred to *T. puercensis* (Fig. 15Y). The paracone and metacone are low and conical with weak paracristid and metacristid. The labial cingulum is pronounced, with a crenulated border bearing several minute cuspules, a small mesostyle, and a prominent parastyle directly anterior to the paracone. There is also a tiny cusp lingual to the mesostyle on the centrocristid. This specimen (L = 7.0 mm) is at the low end of the size range for M1 in *T. puercensis* reported by West (1976; L = 5.9–9.3, n = 57) and Taylor (1984; L = 7.0–9.0, n = 26) for multiple localities they studied.

Although some authors (e.g., Thewissen, 1990) indicate that upper molars of *Tetraclaenodon* lack a mesostyle, Taylor (1984) found that in the collection he studied nearly half (12 of 26 M1 and 9 of 19 M2) have a mesostyle. The small mesostyle on M2 in TxVP 40147-19, referred by Wilson (in Maxwell et al., 1967) and Standhardt (1986) to *T. puercensis*, is much like that in TxVP 41400-30. Hence, although TxVP 41400-34 lacks a mesostyle while TxVP 41400-30 possesses one, their features are otherwise so similar that the two are here referred to the same taxon.

Phenacodus cf. *P. grangeri* Simpson, 1935
Range: Tiffanian (Ti1 through Ti6)

TxVP 40181-1 (Rock Crusher locality) is a fragmentary worn right M2 missing the entire lingual part of the crown and parts of the anterior edge (Fig. 15Z). The crown is broad and quadrangular (L = 10.5+, if complete ~11 mm) with faintly wrinkled enamel and blunt bunodont cusps. The paracone is markedly taller than the metacone; both are only slightly worn. The protocone is mostly broken away, as is the hypocone, and both are worn down to their base. The paraconule is much larger and more severely worn than the metaconule, which lies directly between the metacone and hypocone. There is a very large parastyle; the mesostyle is also very strong and connects the postcingulum to the metacone. The postcingulum extends at least to the base of the hypocone, but its lingual end is broken. Only part of the precingulum is preserved along the base of the paraconule.

This specimen (TxVP 40181-1) is the only one known from the "Rock Crusher" locality (see discussion below). Wilson (p. 104 in Maxwell et al., 1967) initially referred the specimen to *Lambdotherium* sp.; however, subsequently he identified it as *Phenacodus* cf. *P. primaevus* (unpublished note left with specimen dated 1975; see discussion by Lehman et al., p. 27). The very strong parastyle and mesostyle are more like that in *P. matthewi*; however, this is an assessment made primarily on the basis of TxVP 40536-167 (Thewissen, 1990), a specimen that Schiebout (1974) had referred instead to *Ectocion* cf. *E. montanensis*. Although incomplete, 40181-1 is certainly larger than any M2 assigned to *P. matthewi* (L = 7.8–9.3, n = 3; Schiebout, 1974). Its size is in low end of the range for M2 in *P. grangeri* (e.g., L = 10.8–13.3, n = 22; Thewissen, 1990, Cedar Point sample). Given its fragmentary condition, the specimen is assigned here to *Phenacodus* cf. *P. grangeri*.

Maximum Depositional Ages Based on Detrital Zircons

A sample (JC 8) was separated for detrital zircon U-Pb geochronology from the sandstone layer at the top of the "odd conglomerate" bed at the Rough Run East outcrop. This is the same sandstone layer that yielded the charophyte flora described above, and from which the spherule-like grains and quartz grains with planar deformation features also described were collected (Fig. 11; Cobb, 2016). The $^{206}Pb/^{238}U$ age distribution for this detrital zircon sample provides a maximum depositional age estimate for the "odd conglomerate."

Much smaller samples of zircons were also obtained from two mudstone beds (samples KT4 and KTTb) at the Dawson Creek outcrop. These mudstone beds were initially sampled because their low density and light color suggested these could be reworked or altered tuff beds, and the washed sand fraction contained altered glass shards and bipyramidal quartz grains. It is clear, however, from the age distribution of zircons separated from these samples, that these are also detrital assemblages, and therefore provide only estimated maximum depositional ages.

Sample JC 8 ("Odd Conglomerate")

The large sample of zircons (n = 133) obtained from the "odd conglomerate" is remarkably concordant (92%–104%) in the Wetherill U-Pb concordia plot (Table S1, see footnote 1). Thus, no analyses were excluded from the age histogram–KDE plot (Fig. 16) for this sample. Detrital zircons are dominated by $^{206}Pb/^{238}U$ ages between ca. 62 and 97 Ma (114/133 or 86%) and particularly ca. 62 and 69 Ma (76/133 or 57%). Sparse older zircons extend in age to ca. 1680 Ma. The maximum depositional age (MDA) can be estimated from the zircon sample by various methods (Coutts et al., 2019). If the age and uncertainty of the youngest grain measured within the sample provides the MDA and its uncertainty (e.g., Dickinson and Gehrels, 2009), then the $^{206}Pb/^{238}U$ age = 61.9 ± 0.9 ($2\sigma_{prop}$) Ma (Table S1). If the weighted average of the youngest three ages

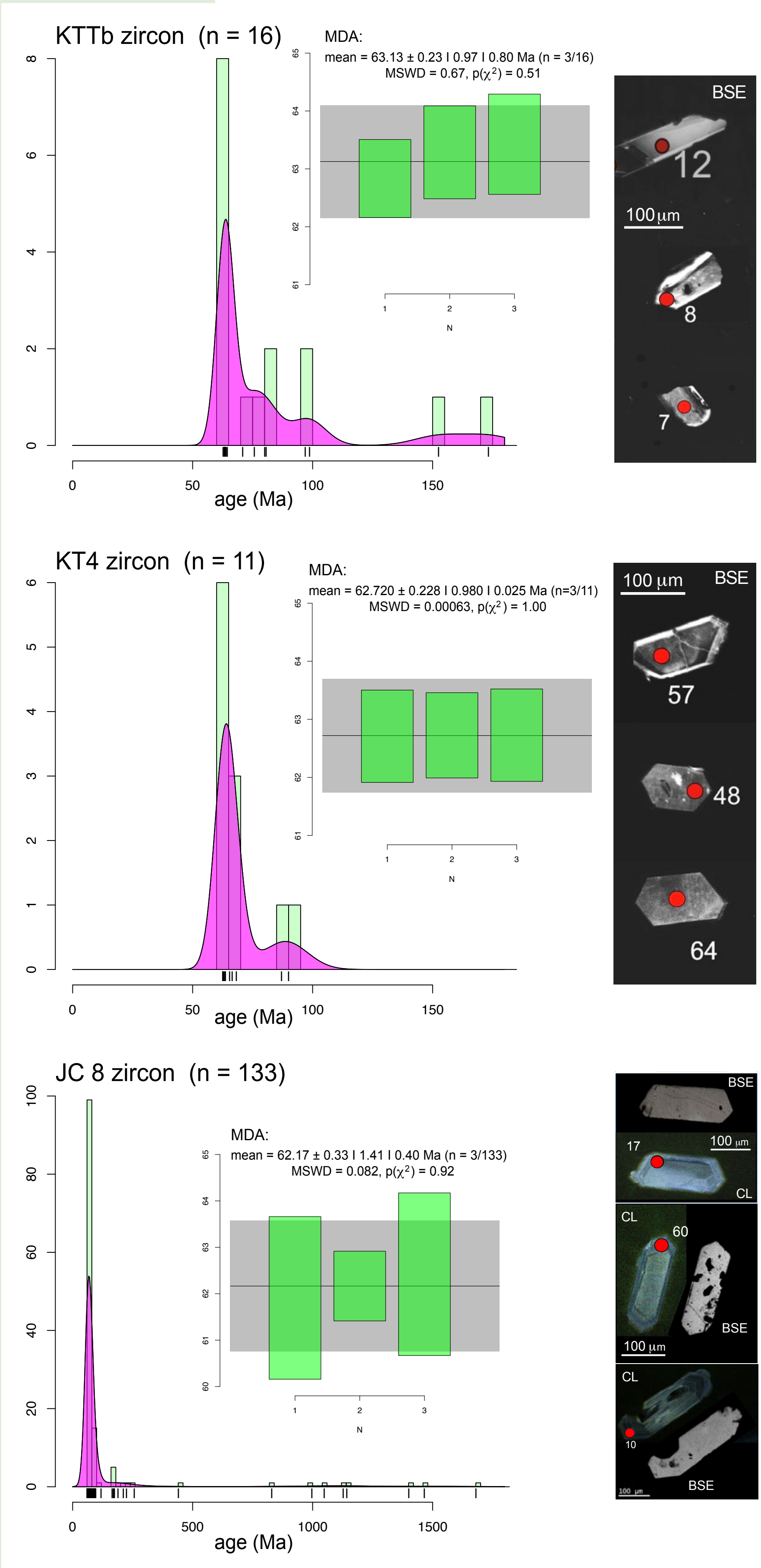

Figure 16. U-Pb detrital zircon age histogram–kernel density estimation (KDE) plots for JC 8 (n = 133 grains with analyses 105%–80% concordant with respect to $^{206}Pb/^{238}U$–$^{207}Pb/^{235}U$ ratios), KT4 (n = 11 concordant analyses), and KTTb (n = 16 concordant analyses) samples from the Dawson Creek outcrop. Kernal and histogram bandwidths are 20 Ma. Insets show the weighted average ages for the three youngest zircon grains for each sample, representing an estimate of the maximum depositional age (MDA). Plots and calculated means for each set of three ages are generated using the *IsoplotR* software (Vermeesch, 2018), where mean = weighted mean age (μ) ± standard error (σ) of μ| ± width of the 100(1-α)% confidence interval for μ| ± approximate 100(1-α)% confidence interval for μ with overdispersion. MSWD—mean square of weighted deviates for age homogeneity; p(χ2) = Chi-squared p-value for the age homogeneity test. At the far right are backscattered electron (BSE) ± cathodoluminescence (CL) images of the three youngest zircon grains, with the laser spot analysis location within each grain indicated by the red dot and associated analysis sequence number.

that overlap with 2σ uncertainty is used (e.g., Zhang et al., 2016), then the $^{206}Pb/^{238}U$ age = 62.17 ± 0.66 (2σ) Ma (Fig. 16).

A dominant mode in the detrital zircon age population falls between 65 and 67 Ma (25/133 or 19%), which generally coincides with the time of the K-Pg boundary event (66 Ma; Renne et al., 2013), and so a large fraction of the zircon population appears to have been reworked from deposits of that age. Lesser modes at ca. 75 Ma and ca. 83 Ma generally coincide with ages of volcanic activity in the Sierra Madre Occidental of western Mexico (e.g., McDowell et al., 2001), a likely source area for sediments of the Tornillo Group (Lehman, 1991).

Sample KT4

Sample KT4 was collected from a mudstone bed 14 m above the "odd conglomerate" at the Dawson Creek outcrop (Fig. 17). This sample, and KTTb discussed below, are dominated by grains >20% discordant with respect to $^{206}Pb/^{238}U$–$^{207}Pb/^{235}U$ ratios. The discordant analyses plot to the right of the Wetherill concordia (Fig. S1, see footnote 1) as positive arrays with low slopes, suggesting the incorporation of variable amounts of common Pb. Thus, for analyses <20% discordant, common Pb corrections were made to the data using the ^{207}Pb method assuming an age-appropriate Pb composition from the Stacey and Kramers (1975) two-stage Pb-evolution model.

For sample KT4, analyses for 11 common Pb–corrected zircon grains were obtained and range in age from ca. 63–90 Ma (Table S2, see footnote 1). If, as above, the age and uncertainty of the youngest grain measured within the sample provide the MDA and its uncertainty, then the common Pb corrected $^{206}Pb/^{238}U$ age = 62.7 ± 0.8 ($2\sigma_{prop}$) Ma. If the weighted average of the youngest three dates that overlap with 2σ uncertainty is used, then the $^{206}Pb/^{238}U$ age = 62.72 ± 0.46 (2σ) Ma (Fig. 16).

Sample KTTb

Sample KTTb was collected from a mudstone bed 1 m above the "Tom's Top" site at the Dawson Creek outcrop (Fig. 17). Only 13 common Pb–corrected, concordant zircon grains were obtained from this sample. Their ages range from ca. 63–99 Ma, with outliers at 153 and 173 Ma (Table S2). If, as above, the age and uncertainty of the youngest grain measured within the sample provides the MDA and its uncertainty, then the common Pb–corrected $^{206}Pb/^{238}U$ age = 62.8 ± 0.7 ($2\sigma_{prop}$) Ma. If the weighted average of the youngest three ages that overlap with 2σ uncertainty is used, then the $^{206}Pb/^{238}U$ age = 63.13 ± 0.46 (2σ) Ma (Fig. 16).

DISCUSSION

The Cretaceous-Paleogene Contact

In all seven areas where the contact between Cretaceous and Paleocene strata can be constrained with biostratigraphically useful fossils, the K-Pg contact lies between the uppermost part of the Javelina Formation and the base of the "log jam sandstone" interval in the Black Peaks Formation, and generally less than 80 m above the top of the Javelina Formation.

In exposures on Dawson Creek and Rough Run Creek the K-Pg contact is marked by the peculiar "odd conglomerate"—a thin bed resting on an erosional surface incised into the underlying strata. Although this bed coincides with the contact between Cretaceous and Paleocene strata, and is superficially similar to deposits elsewhere interpreted as a product of tsunami generated by the Chicxulub impact (e.g., Cobb, 2016), the MDA of ca. 63 Ma reported herein for the "odd conglomerate" indicates that this deposit postdates the Chicxulub impact by several million years. Sand in the "odd conglomerate" includes a few rare grains with planar deformation features and siliceous spherule-like grains with morphologies similar to "splash form" microtektites. While it is possible that these unusual grains were reworked from deposits that originated at the time of the K-Pg boundary impact, there is no compelling evidence for that, and a more mundane pyroclastic origin for these few unusual grains is just as likely.

The "odd conglomerate" appears to represent a thin residual veneer of alluvial deposits that accumulated on the K-Pg disconformity. In most areas, the conglomerate bed is thin, matrix-supported, poorly sorted, weakly stratified, and with large subangular "outsized" clasts (Facies A). These are features commonly associated with deposits resulting from mass-gravity movement such as creep or debris flow (e.g., reviewed by Middleton and Hampton, 1973; Selby, 1993; Miller and Juilleret, 2020). In a few areas, the conglomerate is thicker and is instead clast-supported, better sorted, with rounded clasts, and well stratified in fining-upward beds (Facies B). These are features typical of bedload deposits accumulated by traction transport in channelized watercourses (e.g., reviewed by Miall, 1996). These thicker lenses may represent the fill of small channels cut on the disconformity surface.

In addition to fragmentary dinosaur bones and teeth, the "odd conglomerate" contains a charophyte flora indicative of Maastrichtian age; however, given the ca. 63 Ma MDA estimate, these fossil occurrences must all be a product of reworking from underlying strata and do not convey the actual depositional age of the "odd conglomerate." Occurrences of apparently reworked fossils in both marine and continental K-Pg boundary strata have been a subject of much interest and debate, with some workers arguing for a "conventional" interpretation—that such fossils record exhumation and re-burial of remains derived from Cretaceous strata (e.g., Olsson and Liu, 1993; Arz et al., 2004; Sullivan et al., 2005); others argue, however, that such fossils are not reworked and that the impact horizon therefore preceded the later extinction of Cretaceous taxa (e.g., Keller et al., 2004), or that such fossils record the survival of "Cretaceous" taxa into Paleocene time (e.g., Sloan et al., 1986; Fassett, 2009; Fassett et al., 2010). The MDA assessment reported herein indicates that fossils found in the "odd conglomerate" must certainly be reworked, although the time span separating the original burial of the remains from their later exhumation and re-burial as fossils (~3 million years) seems extraordinary.

The magnitude of the disconformity at the K-Pg contact appears to vary, however, across the

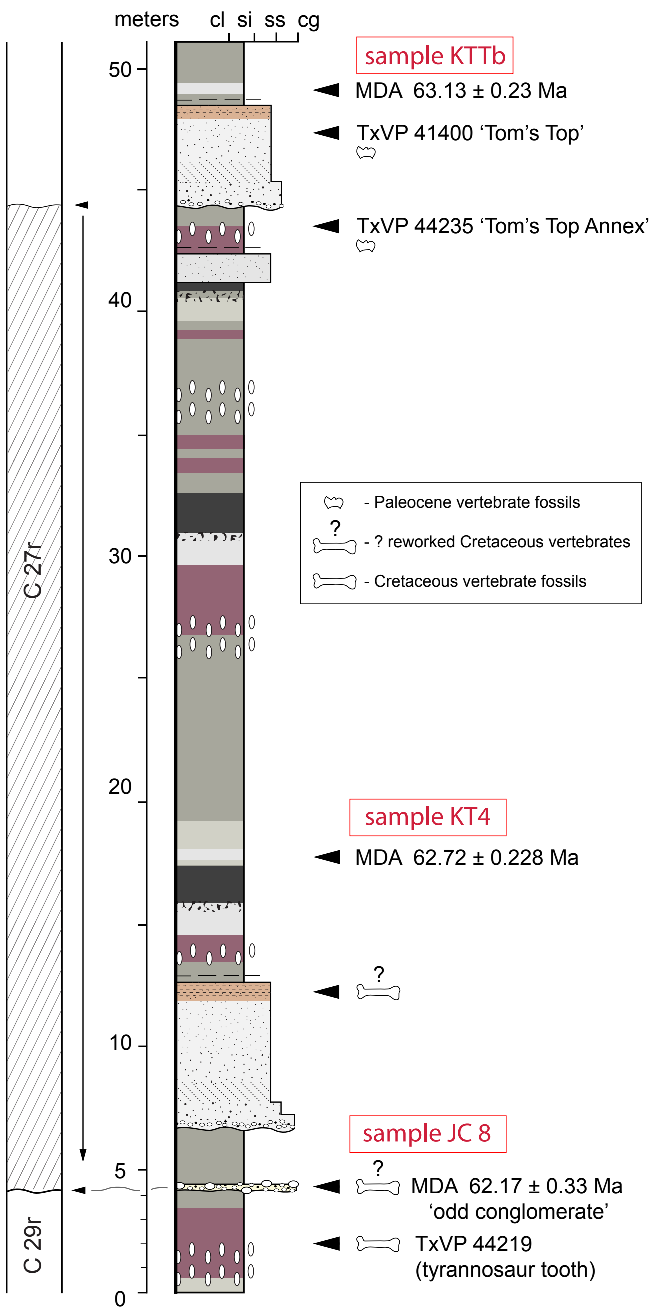

Figure 17. Detailed stratigraphic section of the K-Pg contact interval at the Dawson Creek exposure (section #1 of Fig. 2) showing position of detrital zircon samples relative to sites that yielded uppermost dinosaur specimen considered in situ (not reworked) and sites yielding Paleocene mammals; dinosaur specimens that are probably reworked are indicated with question marks; on left is shown the preferred correlation of magnetic polarity zones for the Dawson Creek section given by Leslie et al. (2018a) with arrow indicating most likely position of disconformity at base of magnetic overprint interval (cross-hatched) rather than top. MDA—maximum depositional age; cl—claystone; si—siltstone; ss—sandstone; cg—conglomerate.

Tornillo Basin from west to east. About 80 m of strata, between the top of the Javelina Formation and base of the "odd conglomerate" are present at Rough Run Creek and at all sites farther east, but these strata are absent at the Dawson Creek exposure, where the "odd conglomerate" is 8 m below the top of the Javelina Formation (Fig. 2). In areas east of Dawson Creek where this intervening 80 m section is preserved, it is largely unfossiliferous; however, at several sites inarguably in situ dinosaur specimens have been collected immediately below the "odd conglomerate" (e.g., TxVP 45891 at Rough Run Amphitheater; see Fig. 2, section #2) or immediately below sites that preserve bonafide Torrejonian mammalian specimens (e.g., TxVP 43621 at Grapevine Hills; see Fig. 2, section #7). These sites indicate that even outside of the Dawson Creek and Rough Run Creek areas, and perhaps everywhere in the Tornillo Basin, early Paleocene strata are absent. Strata of middle Torrejonian (To2) age rest directly on those of late Maastrichtian age. If the upper part of the Javelina Formation at Dawson Creek is correctly correlated with C29r (Leslie et al., 2018a), then the hiatus represented by this disconformity includes the entire Puercan and earliest Torrejonian (To1) interval zones. Moreover, there is no compelling evidence to indicate that the K-Pg boundary event horizon itself is preserved at any of the seven sites, and so some part of latest Maastrichtian time is likely also included in this hiatus as well. The disconformity must therefore span at least 3 million years—from ca. 66–63 Ma.

Age Assessments Based on Mammalian Fauna

All eight of the Paleocene vertebrate fossil sites within the K-Pg contact interval yield mammalian fossils that are compatible with the Torrejonian age assessment that Leslie et al. (2018a) documented for the Tom's Top and Dogie localities. Additional specimens from those localities described herein corroborate that assessment. On the basis of the presence of *Mixodectes malaris* and *Plesiolestes nacimienti* (Tom's Top, TxVP 41400) and *Ellipsodon inaequidens* (Dogie, TxVP 42327), Leslie et al. (2018a) concluded that the Tom's Top and Dogie faunas are correlative with the middle Torrejonian (To2 interval zone). Moreover, mammals recovered at other sites within this interval, *Psittacotherium multifragum* (Cobb's Knob, TxVP 44238) and *Dueterogonodon noletil* (Robber's Roost, TxVP 40151), have first appearances elsewhere also in the middle Torrejonian (e.g., Lofgren et al., 2004), and so it seems likely that this entire stratigraphic interval pertains to the middle Torrejonian (To2 interval zone).

Of the additional taxa reported herein, only TxVP 43380-2 assigned to *Protoselene* cf. *P. griphus* suggests possible correlation instead with the early Torrejonian (To1) inasmuch as this species is thought by some (e.g., Lofgren et al., 2004) to indicate an early Torrejonian age. However, the referral here is a tentative one, and specimens attributed to this species are otherwise so rare that its usefulness for biostratigraphy may be dubious (e.g., Williamson and Lucas, 1992). Viewed collectively, the taxa known from all eight sites are compatible with correlation to the middle Torrejonian (To2 interval zone). All of these sites are from within the stratigraphic interval lying between the top of the "odd conglomerate" and the base of the "log jam sandstone" marker horizon.

The "T2" site (TxVP 40147) is, however, substantially higher (≈40–60 m) than the other eight sites described above, and it is one of only a few sites thus far known from the level of the "log jam sandstone" (Fig. 2, section #8). The "T2" site actually consists of two nearby sites ("Middle Peak" and "Alligator Alley") within 3 m stratigraphically of one another, both within the "log jam sandstone" interval (Fig. 2, section #8). The mammalian fauna from "T2" has been variously interpreted. Wilson (in Maxwell et al., 1967) indicated that the fauna was Torrejonian in age, but Schiebout (1974) and Rapp et al. (1983) suggested a Tiffanian age. Schiebout et al. (1987, their table 1) listed the "T2" fauna as Torrejonian, but elsewhere (their figure 7) indicated a Tiffanian age. Lofgren et al. (2004) argued for a Torrejonian (To2?) age assessment.

Several taxa recorded from the "T2" site (TxVP 40147-34, -64 *Mimetodon silberlingi*, 40147-6, -15, -38, -45, -46, -66, -68 *Baiotomeus douglassi*) make their first appearance in late Torrejonian (To3), others (TxVP 40147-62 *Navajovius kohlhaasae*) a first appearance in early Tiffanian (Ti1; Lofgren et al., 2004). If TxVP 40147-19 is correctly referred to *Tetraclaenodon puercensis* (see Wilson, in Maxwell et al., 1967; Standhardt, 1986), then the site can likely be no younger than the Ti1 interval zone. The "T2" site is certainly higher stratigraphically than any of the sites within the K-Pg contact interval discussed above, and the mammalian fauna here is thus probably latest Torrejonian (To3) to early Tiffanian (Ti1) in age. *Navajovius kohlhaasae* is considered by some to be an index for the early Tiffanian (Ti1; Lofgren et al., 2004), and if so, the "T2" fauna is early Tiffanian (Ti1 interval zone).

Apart from the mammalian taxa represented in the "T2" fauna, confusion regarding this site derives, at least in part, from uncertainty about its stratigraphic position. The "T2" site is at the McKinney Hills outcrop on eastern Tornillo Flat (Fig. 4), ~7 km distant from the type section of the Black Peaks Formation on western Tornillo Flat where the well-studied stratigraphic succession of Tiffanian (Ti1 through Ti5) mammalian faunas described by Schiebout (1974) were collected. Wilson (in Maxwell et al., 1967) indicated that the "T2" site was 43 m above the base of the Black Peaks Formation, and this stratigraphic placement was accepted by Schiebout (1974) as well as subsequent workers. But the position of the lower contact (as it was mapped at that time) differed between the western and eastern sides of Tornillo Flat (see Lehman et al., 2018). The "T2" site is actually lower than all sites on western Tornillo Flat except TxVP 41274 ("C-Con" site of Standhardt, 1986) and 41377 ("Schiebout-Reeves Quarry" of Schiebout, 1974); these sites are not lower than "T2" but are instead at a comparable stratigraphic level (the "log jam sandstone" interval). These sites also yielded a fauna regarded as either latest Torrejonian or earliest Tiffanian age (Schiebout, 1974; Standhardt, 1986). In addition, the "Rock Crusher" site (TxVP 40181), 4 km southwest of "T2" also in the "log jam sandstone," produced a specimen referred here to *Phenacodus* cf. *P. grangeri* (see description above). Although the specimen is fragmentary, it also suggests that the age for this interval is likely Tiffanian, and can be no older than late Torrejonian (To3; Thewissen, 1990; Lofgren et al., 2004).

Collectively, all of the sites thus far known from within or around the "log jam sandstone" interval (TxVp 40147, 40181, 41274, and 41377) are most compatible with an early Tiffanian (Ti1) age assessment. If this is correct, then the latest Torrejonian (To3) interval could be entirely missing in the Black Peaks Formation, and the base of the "log jam sandstone" may coincide with a second intra–Black Peaks disconformity (spanning ~500 k.y.) separating strata bearing a To2 fauna from those bearing a Ti1 fauna.

Moreover, the To2 interval zone occurs within reversed polarity chron C27r, while the To3 interval zone occurs within normal polarity chron C27n (Leslie et al., 2018b; Flynn et al., 2020), and the Ti1 interval zone occurs within reversed polarity chron C26r (Lofgren et al., 2004). The absence of an interval with normal magnetic polarity between strata bearing a To2 fauna and those bearing a Ti1 fauna in either of the paleomagnetic polarity sequences documented for the Black Peaks Formation (Rapp et al., 1983; Leslie et al., 2018a) therefore also accords with the presence of this second intraformational disconformity (Fig. 2).

Maximum Depositional Age Estimates

Maximum depositional ages based on $^{206}Pb/^{238}U$ ages for detrital zircons in the "odd conglomerate" at Rough Run Creek, and for stratigraphic units below and above the Tom's Top locality on Dawson Creek, indicate that the "odd conglomerate" and at least 40 m of overlying strata are no older than 63–62 Ma, an age compatible with the middle Torrejonian age assessment based on the mammalian fauna discussed above (To2 interval zone, ca. 63.5–62.5 Ma; Flynn et al., 2020; Fig. 17). Moreover, the most robust of the MDA determinations (for sample JC 8) also yields the youngest $^{206}Pb/^{238}U$ age of ca. 62 Ma, or considering uncertainty from 60.5 to 62.8 Ma; and this suggests that the Black Peaks Torrejonian mammalian fauna may represent only the later part of the To2 interval zone instead of the earliest part (Flynn et al., 2020).

These MDA estimates indicate that the disconformity Leslie et al. (2018a) hypothesized at the base of the Tom's Top sandstone (194 m level in the section shown in their figure 2) must instead lie ~30 m lower in the section, at the base of the "odd conglomerate" (not shown in their section, but ≈165 m level in their figure 2). Therefore, the entire magnetic overprint interval that they identify below Tom's Top likely also pertains to C27r rather than C29r (Fig. 17).

Bataille et al. (2019; see also Colliver, 2017) also described two detrital zircon samples from the lower part of the type section of the Black Peaks Formation on western Tornillo Flat. The lowermost of their samples (#113015LC-02 of Colliver, 2017) is from a sandstone bed within the K-Pg contact interval. The youngest single zircon grain in this sample yielded a $^{206}Pb/^{238}U$ age of 62.8 ± 1.6 (2σ) Ma, and based on the youngest mode in the age histogram plot, Colliver (2017) estimated the MDA as ca. 64 Ma. This sandstone bed has not produced any diagnostic fossils, and its stratigraphic position relative to the K-Pg contact is uncertain. Its lithology and general stratigraphic level (~50 m above the top of the Javelina Formation) are, however, comparable to the sandstone at the "Hoplochelys Ridge" site nearby at Grapevine Hills (5 km southwest of Tornillo Flat; Fig. 2, section #7). Regardless of its precise correlation, the detrital zircon age distribution and estimated MDA given by Colliver (2017) for the sandstone on Tornillo Flat are quite similar to those reported here for the "odd conglomerate" on Rough Run Creek. Thus, the disconformable relationship between Upper Cretaceous and Paleocene strata documented for the western part of the Park likely applies to the eastern part of the Park as well.

A second detrital zircon sample described by Bataille et al. (2019) is from the "log jam sandstone" interval (sample # 113015LC-03 of Colliver, 2017). The youngest single zircon grain in this sample yielded a $^{206}Pb/^{238}U$ age of 60.6 ± 1.6 (2σ) Ma; however, the age determined for this grain is a distinct outlier in the age distribution. The youngest mode in the age histogram plot is markedly older (72–82 Ma), and therefore, Colliver (2017) estimated the MDA as ca. 79 Ma. Nevertheless, the age of the youngest single grain in the sample is compatible with assessment of the mammalian fauna of the "log jam sandstone" as within the early Tiffanian (Ti1 interval zone; ca. 61–60 Ma, Lofgren et al., 2004) and substantially younger than the underlying part of the Black Peaks Formation (see above).

Origin of the "Odd Conglomerate"

The unusual attributes of the "odd conglomerate" suggest that it records an unusual event that took place during the hiatus represented by the disconformity in the section between ca. 66 and 63 Ma. And yet, this thin bed is so obscure that it has gone largely unnoticed prior to the present work. For example, in the alluvial sequence stratigraphic model Atchley et al. (2004, their figure 3) presented for the Javelina–Black Peaks succession at Dawson Creek, they recognized two sequence boundaries—one within the middle of the Javelina Formation and the other within the middle of the Black Peaks Formation (at 127 and 215 m in their stratigraphic section). Neither of these sequence boundaries coincide with two unconformities that Leslie et al. (2018a; at 100 and 194 m in their figure 2) recognized on the basis of magnetic polarity stratigraphy in the same section. The "odd conglomerate" (not shown but at about the 165 m mark in their stratigraphic section) does not correspond to any of these hypothesized sequence boundaries or unconformities.

Although not recognized by either Atchley et al. (2004) or Leslie et al. (2018a), one plausible interpretation of the "odd conglomerate" is that it coincides with a major stratigraphic sequence boundary resulting from a eustatic fall in sea level. For example, the eustatic cycle chronology of Haq (2014) shows a major early Paleocene sequence boundary ("PaDa3" sea-level fall event) with an estimated peak age of 63.8 Ma. Sedimentation in the Tornillo Basin could have been affected by eustatic sea-level changes. The basin was not closed hydrologically; throughout deposition of the Javelina–Black Peaks succession stream flow was to the southeast, and this fluvial system is presumed to have reached an outlet at sea level, ~300 km away in northeastern Mexico (Lehman et al., 2018; Lehman, 2021).

If the disconformity at the base of the "odd conglomerate" does represent a major stratigraphic sequence boundary, the conglomerate itself could be interpreted as the basal lowstand systems tract (e.g., fluvial channel thalweg deposits of Allen and Posamentier, 1993) within an incised valley system. The "odd conglomerate" bed does occupy the floor of a paleo-valley at the Rough Run East outcrop, or a "paleo-gully," given its small width (800 m, Fig. 9). Incised valley-fill deposits have been widely described in marginal marine settings where they are thought to record relative sea-level fall events and subsequent sea-level highstands that typically result in accumulation of estuarine sedimentary facies (e.g., Dalrymple, 2006 and references cited therein). In contrast, the "odd conglomerate" and overlying strata accumulated in a fully terrestrial environment and would have been entirely within the headward reaches of such an incised valley system, its most landward extent or "segment 3" of Dalrymple et al. (1994).

There are sea-level lowstand deposits that immediately postdate the Chicxulub impact at ca. 66 Ma in the Gulf Coastal Plain of Texas and Mexico (e.g., Keller et al., 2011). However, the eustatic cycle chronology of Haq (2014) indicates that sea-level lowstands of similar magnitude occurred multiple times during accumulation of the Javelina–Black Peaks succession, and if the disconformity at the base of the "odd conglomerate" records such an event, similar deposits should perhaps be more common in the Tornillo Group.

Buried paleo-valley and paleo-gully systems have also been attributed to base-level changes resulting from tectonism (e.g., Kraus and Middleton, 1987; Hippolyte et al., 2011). The westernmost exposure of the K-Pg contact interval at Dawson Creek lies along the flank of a Laramide-age fold, the Terlingua monocline (Erdlac, 1990, 2002; Fig. 3). The "odd conglomerate" is 8 m below the top of the Javelina Formation at Dawson Creek, and ~80 m of strata between the top of the Javelina Formation and base of the "odd conglomerate" are absent here but present at sites farther east (Fig. 2). This may indicate that initial uplift of the Terlingua monocline occurred during early Paleocene time resulting in removal of a substantial section of pre-Torrejonian strata from the Dawson Creek area. Hence, an alternative interpretation is that the disconformity overlain by the "odd conglomerate" resulted from local tectonism rather than eustatic sea-level change.

Relationship to the Terlingua Monocline

Strata along the south flank the Terlingua monocline are deformed within the limb of the fold and dip steeply to the south (Fig. 3). Therefore, most of the deformation here must have taken place after deposition of the Tornillo Group. However, in addition to the relief on the "odd conglomerate" disconformity, several observations (enumerated below) suggest that this fold began to form earlier during deposition of the Tornillo Group.

(1) The Javelina Formation at Dawson Creek is thinner than is typical of exposures farther east. For example, as these strata are currently mapped (Turner et al., 2011), the Javelina Formation at Dawson Creek is 123 m (Lehman et al., 2018) to 133 m thick (Leslie et al., 2018a). In contrast, a typical section exposed farther east, on Tornillo Flat, has a thickness of 170–180 m (e.g., Lehman et al., 2018; their figure 6).

(2) The Javelina Formation at Dawson Creek exhibits sedimentary facies that differ from those typical of the formation farther east. For example, the section on northern Tornillo Flat (Lehman et al., 2018; their figure 6) includes significant lacustrine facies that are absent on Dawson Creek, as well as a greater proportion of mudstone, and fewer well-differentiated paleosols (see also Lehman, 2021).

(3) The middle and upper parts of the Black Peaks Formation are entirely missing along the Terlingua monocline, truncated at the base of the overlying Canoe Formation. For example, on Tornillo Flat, the Black Peaks Formation is in excess of 300 m thick, whereas on Dawson Creek, it is only ~70 m thick (Lehman et al., 2018). Only the lower part of the formation (below the level of the "log jam sandstone" marker bed of Lehman and Busbey, 2007) is present on Dawson Creek.

Collectively, these local differences in the Tornillo Group section at Dawson Creek indicate that this was an area subject to uplift and erosion, or one that experienced lower sedimentation rates compared to nearby areas elsewhere in the Tornillo Basin. Although the culmination of Laramide deformation must have occurred during early to middle Eocene time (Lehman et al., 2018), a plausible explanation for the local peculiarities in the Tornillo Group section at Dawson Creek is that uplift of the Terlingua monocline began earlier during deposition of the Javelina and Black Peaks formations. The spatial association of the "odd conglomerate" with the Dawson and Rough Run Creek vicinity suggests that the disconformity at its base was a result of local tectonism. The disconformal relationship between Cretaceous and Paleocene strata throughout the Tornillo Basin may therefore reflect base-level change due to a tectonic rather than eustatic mechanism.

Terrestrial K-Pg Boundary Sites in North America

At multiple localities in the northern Great Plains and Rocky Mountains of western Canada, North Dakota, Montana, Wyoming, and Colorado, the K-Pg impact horizon has been identified and a relatively complete and detailed record of terrestrial faunal turnover at the K-Pg boundary is preserved (e.g., reviewed by Lillegraven and Eberle, 1999; Lofgren et al., 2004; Dahlberg et al., 2016). In all of these areas, the latest Cretaceous (Lancian) '*Triceratops* fauna' is succeeded by an earliest Puercan (Pu1 interval zone) mammalian fauna.

In contrast, at sites spanning the K-Pg contact interval throughout southwestern North America, the latest Cretaceous (Lancian) vertebrate assemblage is instead typified by the so-called '*Alamosaurus* fauna' (e.g., Lehman et al., 2006); and at these sites, in the Wasatch Basin of Utah (e.g., Cross and Yi, 1997) and in the San Juan Basin of New Mexico (e.g., Clemens and Williamson, 2005), the K-Pg impact horizon has not been identified, and an earliest Puercan (Pu1 interval zone) has not been documented (Lofgren et al., 2004; Flynn et al., 2020). It appears that the same is true in the Tornillo Basin of West Texas, where the magnitude of the disconformity separating Cretaceous and Paleocene strata is even greater than in New Mexico and Utah. Hence, there is a hiatus that spans some part of latest Cretaceous and earliest Paleocene time in the terrestrial stratigraphic record throughout part or all of southwestern North America. Consequently, there is thus far no way to know whether the terrestrial extinction and recovery here was manifested in a way similar to that documented in the northern interior biome of North America.

CONCLUSIONS

The K-Pg contact interval in the Tornillo Group is constrained by vertebrate fossil sites at seven localities in Big Bend National Park and lies within an ~80–100 m stratigraphic section between the top of the Javelina Formation and the base of the "log jam sandstone" marker horizon in the Black Peaks Formation. In western exposures of this interval, the highest occurrence of in situ dinosaur specimens and the lowest occurrence of Paleocene mammal specimens are separated by an unusual conglomerate bed. This thin conglomerate bed represents a residual alluvial deposit that accumulated on an erosional surface. The "odd conglomerate" coincides with the contact between Cretaceous and Paleocene strata, contains Cretaceous fossils, and is superficially similar to conglomerate beds elsewhere attributed to the effects of tsunamis generated by the Chicxulub impact. However, the maximum depositional age of ca. 63 Ma established on the basis of detrital zircons indicates that the "odd conglomerate" bed was deposited ~3 million years after the K-Pg boundary event. Although occurrences elsewhere of Cretaceous fossils within what otherwise appear to be Paleocene strata have been a subject of varied interpretation and debate; in this case, the fossils are believed to have been exhumed from Cretaceous strata and reworked prior to preservation in Paleocene strata.

At all seven sites where the K-Pg contact interval is documented, Paleocene mammalian fossils from immediately above the "odd conglomerate" represent a fauna of Torrejonian age, and most or all of these sites can be no older than the middle Torrejonian (To2 interval zone). No sites yielding a

Puercan or early Torrejonian fauna have been discovered, and so the contact between Cretaceous and Paleocene strata is therefore disconformal and represents a hiatus of at least ~3 million years. The magnitude of this hiatus varies; in the westernmost exposure of the K-Pg boundary interval at Dawson Creek, at least ~80 m of strata are absent below the "odd conglomerate" that are present nearby to the east on Rough Run Creek. The condensed section at Dawson Creek likely records initial uplift and deformation of the Terlingua monocline. Although the ~80 m stratigraphic interval below the "odd conglomerate" east of Dawson Creek is poorly fossiliferous, it has yielded several clearly in situ dinosaur specimens that indicate the entire interval is likely Late Cretaceous in age. As a result, there is no compelling evidence for preservation of the K-Pg boundary event horizon at any of the sites in the Tornillo Group, and so the hiatus represented at the Cretaceous-Paleocene contact here likely includes some part of latest Cretaceous time as well.

Mammalian specimens from vertebrate fossil sites in the "log jam sandstone,"~40 m above the middle Torrejonian sites, instead represent an early Tiffanian fauna (Ti1 interval zone). Latest Torrejonian (To3) sites have not been recognized, and the interval of normal magnetic polarity (chron C27n) that elsewhere in North America bears a latest Torrejonian (To3) fauna, has not been identified in either of the two paleomagnetic polarity sections thus far documented for the Black Peaks Formation. Therefore, a second disconformity likely coincides with the base of the "log jam sandstone" marker horizon in the Black Peaks Formation.

ACKNOWLEDGMENTS

The late J. "Doc" Wilson conducted the original investigation of the K-Pg contact in the Tornillo Group in the 1960s, and subsequent work has mostly verified his early conclusions. D. Lawson and R. Rainey discovered the important "Tom's Top" and "Dogie" localities, essential to all subsequent studies given the rarity of such sites in the Black Peaks Formation. The current report includes results of J. Cobb's M.S. thesis research conducted under the supervision of T. Lehman at Texas Tech University. D. Triplehorn, C. Barnes, and M. Barnes assisted with the preparation and analysis of several of the detrital zircon samples. J. Cottle (University of California, Santa Barbara) supervised the U-Pb zircon dating of samples KT4 and KTTb and provided information about the data acquisition and processing. We thank D. Corrick in the Division of Science and Resource Management at Big Bend National Park for his support of our work in the Park, J. Sagebiel and M. Brown at the Jackson School Museum of Earth Sciences, University of Texas at Austin for their help with specimen curation and continued support of our research. Sharp-eyed fossil collectors T. Shiller, S. Wick, and A. Brink are responsible for spotting most of the rare mammal teeth illustrated in this report, and W. Straight, A. Coulson, T. King, and J. Browning assisted with work at the "Hoplochelys Ridge" and "Yellow Hill" sites that formed the initial basis for the current study. Thoughtful comments and advice from D. Fastovsky and two anonymous reviewers helped to substantially improve the content and presentation of the manuscript.

APPENDIX. SITE NUMBERS AND STRATIGRAPHIC LEVELS

During the course of this investigation, an attempt was made to relocate many of the vertebrate fossil sites within the K-Pg contact interval described by previous workers, and to determine the stratigraphic positions of these sites as accurately as possible. Because the revised age constraints presented here and those given recently by Leslie et al. (2018a) will be useful in future biostratigraphic assessments of Upper Cretaceous and Paleocene terrestrial strata, the identity and stratigraphic positions of these sites may ultimately prove significant, and it is useful to note here several inaccuracies in previous reports and changes in site numbering.

Leslie et al. (2018a, their figure 2) identify and show the stratigraphic positions of important vertebrate fossil sites in the Dawson Creek section, several of which were first described by Lawson (1972). Most of these sites were initially assigned to a single locality number, but subsequently it was recognized that the sites occur at different stratigraphic levels and so were given different numbers.

Locality 6 shown by Leslie et al. (2018a; their figure 2) is identified as TMM (= TxVP) 41501. This number was used in Lawson's (1972) initial study of what would later be designated the holotype specimen of *Quetzalcoatlus northropi*, and the same number was subsequently repeated by Standhardt (1986) and Lehman (1990), but this number is invalid. The correct number for this site is TxVP 41450, and the holotype specimen is 41450-3. The correct stratigraphic level of this site is slightly lower than what is shown by Leslie et al. (2018a; their figure 2), and should be near the base of the sandstone at the 163 m level. Lehman et al. (2018, their appendix I, section #1) also incorrectly showed TxVP 41450 at the base of unit 9 in their section; the site is actually lower—at the base of their unit 7.

Locality 3 shown by Leslie et al. (2018a; their figure 2) is identified as TMM 41450. Although the specimen from this site is a right ulna of *Alamosaurus sanjuanensis* initially described by Lawson (1972) using the number TMM 41450-2, the correct number for this site is TxVP 42426, and the specimen is 42426-1. The stratigraphic level for this site is at the top of the sandstone unit shown at the ~145 m level by Leslie et al. (2018a; their figure 2). Another specimen described by Lawson (1972) from this area is a caudal vertebra assigned to *Alamosaurus sanjuanensis* and given the number TMM 41450-1. The correct number for this specimen is TxVP 42425-1, and its stratigraphic position is at the ~100 m level near locality 2 shown by Leslie et al. (2018a; their figure 2).

Lehman et al. (2018, their appendix I, section #14) identified the "Hoplochelys Ridge" site in the Grapevine Hills section using the number TxVP 43621-2 (the same site number assigned to the juvenile *Alamosaurus* specimen 43621-1, which is 2 m lower stratigraphically); however, the "Hoplochelys Ridge" site was subsequently given its own locality number, TxVP 44234. Lehman et al. (2018, their appendix I, section #16) also incorrectly located the "T-10" site (TxVP 40151) in unit 5 of their "Glenn Springs West" section, but this site is instead lower, within unit 2 of that section.

REFERENCES CITED

Allen, G.P., and Posamentier, H.W., 1993, Sequence stratigraphy and facies model of an incised valley fill; the Gironde Estuary, France: Journal of Sedimentary Research, v. 63, p. 378–391, https://doi.org/10.1306/D4267B09-2B26-11D7-8648000102C1865D.

Archibald, J.D., 1998, Archaic ungulates ("Condylarthra"), *in* Janis, C.M., Scott, K.M., and Jacobs, L.L., eds., Evolution of Tertiary Mammals of North America: Volume 1, Terrestrial Carnivores, Ungulates, and Ungulatelike Mammals: Cambridge, UK, Cambridge University Press, p. 292–331.

Arz, J.A., Alegret, L., and Arenillas, I., 2004, Foraminiferal biostratigraphy and paleoenvironmental reconstruction at the Yaxcopoil-1 drill hole, Chicxulub crater, Yucatan Peninsula: Meteoritics & Planetary Science, v. 39, p. 1099–1111, https://doi.org/10.1111/j.1945-5100.2004.tb01131.x.

Atchley, S.C., Nordt, L.C., and Dworkin, S.I., 2004, Eustatic control on alluvial sequence stratigraphy: A possible example from the Cretaceous-Tertiary transition of the Tornillo Basin, Big Bend National Park, West Texas, U.S.A.: Journal of Sedimentary Research, v. 74, no. 3, p. 391–404, https://doi.org/10.1306/102203740391.

Bataille, C.P., Watford, D., Ruegg, S., Lowe, A., and Bowen, G.J., 2016, Chemostratigraphic age model for the Tornillo Group: A possible link between fluvial stratigraphy and climate: Palaeogeography, Palaeoclimatology, Palaeoecology, v. 457, p. 277–289, https://doi.org/10.1016/j.palaeo.2016.06.023.

Bataille, C.P., Ridgway, K.D., Colliver, L., and Liu, X.-M., 2019, Early Paleogene regime shift in response to global warming: A subtropical record from the Tornillo Basin, west Texas, USA: Geological Society of America Bulletin, v. 131, no. 1–2, p. 299–317, https://doi.org/10.1130/B31872.1.

Bourgeois, J., Hansen, T.A., Wiberg, P.L., and Kauffman, E.G., 1988, A tsunami deposit at the Cretaceous–Tertiary boundary in Texas: Science, v. 241, p. 567–570, https://doi.org/10.1126/science.241.4865.567.

Clemens, W.A., and Williamson, T.E., 2005, A new species of *Eoconodon* (Triisodontidae, Mammalia) from the San Juan Basin, New Mexico: Journal of Vertebrate Paleontology, v. 25, p. 208–213, https://doi.org/10.1671/0272-4634(2005)025[0208:ANSOET]2.0.CO;2.

Clyde, W.C., Ramezani, J., Johnson, K.R., Bowring, S.A., and Jones, M.M., 2016, Direct high-precision U-Pb geochronology of the end-Cretaceous extinction and calibration of Paleocene astronomical timescales: Earth and Planetary Science Letters, v. 452, p. 272–280, https://doi.org/10.1016/j.epsl.2016.07.041.

Cobb, J., 2016, Sedimentology of the Cretaceous-Paleogene boundary interval in the Tornillo Group of West Texas [M.S. thesis]: Lubbock, Texas Tech University, 161 p.

Colliver, L., 2017, Long-term record of sediment transport and deposition at the crossroads of North America's orogenic systems, West Texas, U.S.A.: A detrital zircon view [MS thesis]: West Lafayette, Indiana, Purdue University, 294 p.

Cope, E.D., 1876, On the Taeniodonta, a new group of Eocene mammals: Proceedings of the National Academy of Sciences Philadelphia, v. 28, p. 39.

Cope, E.D., 1881, Mammalia of the lower Eocene beds: American Naturalist, v. 15, p. 337–338.

Cope, E.D., 1882, A new genus of Tillodonta: American Naturalist, v. 16, p. 156–157.

Cope, E.D., 1884, The Tertiary Marsupialia: American Naturalist, v. 18, p. 686–697, https://doi.org/10.1086/273711.

Cope, E.D., 1887, The marsupial genus *Chirox*: American Naturalist, v. 21, p. 566–567.

Coutts, D.S., Matthews, W.A., and Hubbard, S.M., 2019, Assessment of widely used methods to derive depositional ages from detrital zircon populations: Geoscience Frontiers, v. 10, p. 1421–1435, https://doi.org/10.1016/j.gsf.2018.11.002.

Cross, A.T., and Yi, M.S., 1997, Palynology and a review of vertebrate faunas of the Late Cretaceous–Paleocene North Horn Formation, Price Canyon, Wasatch Plateau and environs, Utah, U.S.A., *in* Wolberg, D., and Stump, E., eds., Dinofest International, Proceedings of a Symposium Sponsored by Arizona State University: Philadelphia Academy of Natural Sciences, Special Publication, p. 417–455.

Dahlberg, E.L., Eberle, J.J., Sertich, J.W., and Miller, I.M., 2016, A new earliest Paleocene (Puercan) mammalian fauna from Colorado's Denver Basin, U.S.A.: Rocky Mountain Geology, v. 51, p. 1–22, https://doi.org/10.2113/gsrocky.51.1.1.

Dalrymple, R.W., 2006, Incised valleys in time and space: An introduction to the volume and an examination of the controls on valley formation and filling, *in* Dalrymple, R.W., Leckie, D.A., and Tillman, R.W., eds., Incised Valleys in Time and Space: SEPM (Society for Sedimentary Geology) Special Publication 85, p. 5–12, https://doi.org/10.2110/pec.06.85.0005.

Dalrymple, R.W., Boyd, R., and Zaitlin, B.A., 1994, History of research, types and internal organization of incised-valley systems: Introduction to the volume, *in* Dalrymple, R.W., Boyd, R., and Zaitlin, B.A., eds., Incised-Valley Systems: Origin and Sedimentary Sequences: SEPM (Society for Sedimentary Geology) Special Publication 51, p. 3–10.

Denne, R.A., Scott, E.D., Eickhoff, D.P., Kaiser, J.S., Hill, R.J., and Spaw, J.M., 2013, Massive Cretaceous–Paleogene boundary deposit, deep-water Gulf of Mexico: New evidence for widespread Chicxulub-induced slope failure: Geology, v. 41, p. 983–986, https://doi.org/10.1130/G34503.1.

Dickinson, W., and Gehrels, G., 2009, U-Pb ages of detrital zircons in Jurassic eolian and associated sandstones of the Colorado Plateau: Evidence for transcontinental dispersal and intraregional recycling of sediment: Geological Society of America Bulletin, v. 121, no. 3–4, p. 408–433, https://doi.org/10.1130/B26406.1.

Erdlac, R.J., 1990, A Laramide push-up block, the structures and formation of the Terlingua-Solitario structural block, Big Bend region, Texas: Geological Society of America Bulletin, v. 102, no. 8, p. 1065–1076, https://doi.org/10.1130/0016-7606(1990)102<1065:ALAPUB>2.3.CO;2.

Erdlac, R.J., 2002, The Terlingua Monocline, *in* White, J.C., ed., The Geology of Big Bend National Park: What have we learned since Maxwell and others (1967): Geological Society of America, South-Central Section Meeting, 2002 Field Trip Guidebook, p. 12–14.

Fassett, J.E., 2009, New geochronologic and stratigraphic evidence confirms the Paleocene age of the dinosaur-bearing Ojo Alamo Sandstone and Animas Formation in the San Juan Basin, New Mexico and Colorado: Palaeontologia Electronica, v. 12, 12.13A.

Fassett, J.E., Heaman, L.M., and Simonetti, A., 2010, Direct U-Pb dating of Cretaceous and Paleocene dinosaur bones, San Juan Basin, New Mexico: Geology, v. 39, p. 159–162, https://doi.org/10.1130/G31466.1.

Flynn, A.G., Davis, A.J., Williamson, T.E., Heizler, M.T., Fenley, C.W., Leslie, C.E., Secord, R., Brusatte, S.L., and Peppe, D.J., 2020, Early Paleocene magnetostratigraphy and revised biostratigraphy of the Ojo Alamo Sandstone and lower Nacimiento Formation, San Juan Basin, New Mexico, USA: Geological Society of America Bulletin, v. 132, no. 9–10, p. 2154–2174, https://doi.org/10.1130/B35481.1.

Folk, R.L., 1980, Petrology of Sedimentary Rocks: Austin, Texas, Hemphill Publishing Company, 182 p.

Fouch, T.D., Hanley, J.H., Forester, R.M., Keighin, C.W., Pitman, J.K., and Nichols, D.J., 1987, Chart showing lithology, mineralogy, and paleontology of the nonmarine North Horn Formation and Flagstaff Member of the Green River Formation, Price Canyon, Central Utah: A principal reference section: U.S. Geological Survey, Miscellaneous Investigations Map I-1797-A.

Fronimos, J.A., and Lehman, T.M., 2014, New specimens of a titanosaur sauropod from the Maastrichtian of Big Bend National Park, Texas: Journal of Vertebrate Paleontology, v. 34, p. 883–899, https://doi.org/10.1080/02724634.2014.840308.

Fuentes, A.J., Clyde, W.C., Weissenburger, K., Bercovici, A., Lyson, T.R., Miller, I.M., Ramezani, J., Schmitz, M.D., and Johnson, K.R., 2019, Constructing a timescale of biotic recovery across the Cretaceous–Paleogene boundary, Corral Bluffs, Denver Basin, Colorado: Rocky Mountain Geology, v. 54, p. 133–153, https://doi.org/10.24872/rmgjournal.54.2.133.

Gazin, C.L., 1939, A further contribution to the Dragon Paleocene of central Utah: Journal of the Washington Academy of Sciences, v. 29, p. 272–286.

Giebel, C., 1855, Odontographie. Vergleichende Darstellung des Zahnsystemes der lebenden und fossilen Wirbelthiere: Leipzig Verlag, 118 p.

Glass, B.P., 1990, Tektites and microtektites: Key facts and inferences: Tectonophysics, v. 171, p. 393–404, https://doi.org/10.1016/0040-1951(90)90112-L.

Grambast, L., 1971, Remarques phylogenetiques et biochronologiques sur les *Septorella* du Cretace terminal de Provence et les charophytes associees: Paleobiologie Continentale, v. 2, p. 1–38.

Gulick, S.P., Bralower, T.J., Ormö, J., Hall, B., Grice, K., Schafer, B., Lyons, S., Freeman, K.H., Morgan, J.V., Artemieva, N., Kaskes, P., de Graff, S.J., Whalen, M.T., Collins, G.S., Tikoo, S.M., Verhagen, C., Christeson, G.L., Claeys, P., Coolen, M.J., Goderis, S., Goto, K., Grieve, R.A., McCall, N., Osinski, G.R., Rae, A.S., Riller, U., Smit, J., Vajda, V., and Wittmann, A., and the Expedition 364 Scientists, 2019, The first day of the Cenozoic: Proceedings of the National Academy of Sciences of the United States of America, v. 116, p. 19,342–19,351, https://doi.org/10.1073/pnas.1909479116.

Haq, B.U., 2014, Cretaceous eustacy revisited: Global and Planetary Change, v. 113, p. 44–58, https://doi.org/10.1016/j.gloplacha.2013.12.007.

Hartman, J.H., Johnson, K.R., and Nichols, D.J., 2002, The Hell Creek Formation and the Cretaceous-Tertiary Boundary in the Northern Great Plains: Geological Society of America Special Paper 361, 520 p., https://doi.org/10.1130/SPE361.

Hippolyte, J.C., Clauzon, G., and Suc, J.P., 2011, Messinian-Zanclean canyons in the Dine nappe (southwestern Alps): Tectonic implications: Bulletin de la Société Géologique de France, v. 182, p. 111–132, https://doi.org/10.2113/gssgfbull.182.2.111.

Keller, G., Adatte, T., Stinnesbeck, W., Rebolledo-Vieyra, M., Urrutia Fucugauchi, J., Kramar, U., and Stuben, D., 2004, Chicxulub impact predates the K-T boundary mass extinction: Proceedings of the National Academy of Sciences of the United States of America, v. 101, p. 3753–3758, https://doi.org/10.1073/pnas.0400396101.

Keller, G., Abramovich, T., Adatte, T., and Berner, Z., 2011, Biostratigraphy, age of the Chicxulub impact, and depositional environment of the Brazos River KTB sequences, *in* Keller, G., and Adatte, T., eds., The End-Cretaceous Mass Extinction and the Chicxulub Impact in Texas: SEPM (Society for Sedimentary Geology) Special Publication 100, p. 81–122, https://doi.org/10.2110/sepmsp.100.081.

Knauss, G., Joyce, W.G., Lyson, T.R., and Pearson, D., 2011, A new kinosternoid from the Late Cretaceous Hell Creek Formation of North Dakota and the origin of the *Dermatemys mawii* lineage: Palaontologische Zeitschrift, v. 85, p. 125–142, https://doi.org/10.1007/s12542-010-0081-x.

Koch, E., and Blissenbach, E., 1960, Die gefalteten oberkretazisch-tertiaren Rotschichten im Mittel-Ucayali Gebiet, Ostperu: Geologisches Jahrbuch: Beihefte, v. 43, p. 1–103.

Kraus, M.J., and Middleton, L.T., 1987, Dissected paleotopography and base-level changes in a Triassic fluvial sequence: Geology, v. 15, no. 1, p. 18–21, https://doi.org/10.1130/0091-7613(1987)15<18:DPABCI>2.0.CO;2.

Langston, W., Standhardt, B., and Stevens, M., 1989, Fossil vertebrate collecting in the Big Bend—History and retrospective, *in* Busbey, A.B., and Lehman, T.M., eds., Vertebrate paleontology, biostratigraphy, and depositional environments, latest Cretaceous and Tertiary, Big Bend area, Texas: Society of Vertebrate Paleontology, 49th Annual Meeting Fieldtrip Guidebook, p. 11–21.

Lawson, D.A., 1972, Paleoecology of the Tornillo Formation, Big Bend National Park, Texas [M.S. thesis]: Austin, University of Texas at Austin, 182 p.

Lawton, T.F., Shipley, K.W., Aschoff, J.L., Giles, K.A., and Vega, F.J., 2005, Basinward transport of Chixulub ejecta by tsunami-induced backflow, La Popa basin, northeastern Mexico, and its implications for distribution of impact-related deposits flanking the Gulf of Mexico: Geology, v. 33, p. 81–84, https://doi.org/10.1130/G21057.1.

Lehman, T.M., 1985, Stratigraphy, sedimentology, and paleontology of Late Cretaceous (Campanian-Maastrichtian) sedimentary rocks in Trans-Pecos Texas [Ph.D. thesis]: Austin, University of Texas at Austin, 310 p.

Lehman, T.M., 1988, Stratigraphy of the Cretaceous–Tertiary and Paleocene-Eocene transition rocks of Big Bend [discussion]: The Journal of Geology, v. 96, p. 627–631, https://doi.org/10.1086/629258.

Lehman, T.M., 1989, Upper Cretaceous (Maastrichtian) paleosols in Trans-Pecos Texas: Geological Society of America Bulletin, v. 101, p. 188–203, https://doi.org/10.1130/0016-7606(1989)101<0188:UCMPIT>2.3.CO;2.

Lehman, T.M., 1990, Paleosols and the Cretaceous/Tertiary transition in the Big Bend region of Texas: Geology, v. 18, no. 4, p. 362–364, https://doi.org/10.1130/0091-7613(1990)018<0362:PATCTT>2.3.CO;2.

Lehman, T.M., 1991, Sedimentation and tectonism in the Laramide Tornillo Basin of West Texas: Sedimentary Geology, v. 75, no. 1–2, p. 9–28, https://doi.org/10.1016/0037-0738(91)90047-H.

Lehman, T.M., 2002, Revisions to the Tornillo Group (Upper Cretaceous-Eocene), Big Bend National Park, Texas: Geological Society of America, Abstracts with Programs, v. 34, no. 3, p. A10.

Lehman, T.M., 2004, Mapping of Upper Cretaceous and Paleogene strata in Big Bend National Park, Texas: Geological Society of America, Abstracts with Programs, v. 36, no. 5, p. A129.

Lehman, T.M., 2007, Upper Cretaceous and Paleogene strata south of the Chisos Mountains, Big Bend National Park, Texas: Geological Society of America, Abstracts with Programs, v. 39, p. A510.

Lehman, T.M., 2021, Habitat of the giant pterosaur *Quetzalcoatlus* Lawson 1975 (Pterodactyloidea: Azhdarchoidea): A paleoenvironmental reconstruction of the Javelina Formation (Upper Cretaceous) Big Bend National Park, Texas, *in* Padian, K. and Brown, M., eds., The Late Cretaceous pterosaur *Quetzalcoatlus* Lawson 1975: Society of Vertebrate Paleontology Memoir 19, p. 21–45, https://doi.org/10.1080/02724634.2019.1593184.

Lehman, T.M., and Busbey, A.B., 2007, Big Bend Field Trip Guidebook: Society of Vertebrate Paleontology, 69 p.

Lehman, T.M., and Coulson, A.B., 2002, A juvenile specimen of the sauropod dinosaur *Alamosaurus sanjuanensis* from the Upper Cretaceous of Big Bend National Park, Texas: Journal of Paleontology, v. 76, p. 156–172, https://doi.org/10.1666/0022-3360(2002)076<0156:AJSOTS>2.0.CO;2.

Lehman, T.M., McDowell, F., and Connelly, J., 2006, First isotopic (U-Pb) age for the Late Cretaceous *Alamosaurus* vertebrate fauna of West Texas, and its significance as a link between two faunal provinces: Journal of Vertebrate Paleontology, v. 26, p. 922–928, https://doi.org/10.1671/0272-4634(2006)26[922:FIUAFT]2.0.CO;2.

Lehman, T.M., Wick, S.L., and Wagner, J.R., 2016, Hadrosaurian dinosaurs from the Maastrichtian Javelina Formation, Big Bend National Park, Texas: Journal of Paleontology, v. 90, p. 333–356, https://doi.org/10.1017/jpa.2016.48.

Lehman, T.M., Wick, S.L., Beatty, H.L., Straight, W.H., and Wagner, J.R., 2018, Stratigraphy and depositional history of the Tornillo Group (Upper Cretaceous–Eocene) of West Texas: Geosphere, v. 14, no. 5, https://doi.org/10.1130/GES01641.1.

Leslie, C., Peppe, D., Williamson, T., Bilardello, D., Heizler, M., Secord, R., and Leggett, T., 2018b, High-resolution magnetostratigraphy of the upper Nacimiento Formation, San Juan Basin, New Mexico, USA: Implications for basin evolution and mammalian turnover: American Journal of Science, v. 318, p. 300–334, https://doi.org/10.2475/03.2018.02.

Leslie, C.E., Peppe, D.J., Williamson, T.E., Heizler, M., Jackson, M., Atchley, S.C., Nordt, L., and Standhardt, B., 2018a, Revised age constraints for Late Cretaceous to early Paleocene terrestrial strata from the Dawson Creek section, Big Bend National Park, west Texas: Geological Society of America Bulletin, v. 130, no. 7–8, p. 1143–1163, https://doi.org/10.1130/B31785.1.

Lillegraven, J.A., and Eberle, J.J., 1999, Vertebrate faunal changes through Lancian and Puercan time in southern Wyoming: Journal of Paleontology, v. 73, p. 691–710, https://doi.org/10.1017/S0022336000032510.

Lofgren, D.L., Lillegraven, J.A., Clemens, W.A., Gingerich, P.D., and Williamson, T.E., 2004, Paleocene biochronology: The Puercan through Clarkforkian Land Mammal Ages, *in* Woodburne, M.O., ed., Late Cretaceous and Cenozoic Mammals of North America: New York, Columbia University Press, p. 43–105, https://doi.org/10.7312/wood13040-005.

Lyson, T.R., Miller, M., Bercovici, D., Weissenberger, K., Fuentes, J., Clyde, C., Hagadorn, W., Butrim, J., Johnson, R., Fleming, F., Barclay, S., MacCracken, A., Lloyd, B., Wilson, P., Krause, W., and Chester, S.G.B., 2019, Exceptional continental record of biotic recovery after the Cretaceous-Paleogene mass extinction: Science, v. 366, p. 977–983, https://doi.org/10.1126/science.aay2268.

Mahaney, W.C., 2002, Atlas of Sand Grain Surface Textures and Applications: Oxford, UK, Oxford University Press, 237 p.

Marsh, O.C., 1876, Notice of new Tertiary mammals: American Journal of Science, 3rd Series, v. 12, p. 401–404.

Matthew, W.D., 1937, Paleocene faunas of the San Juan Basin, New Mexico: Transactions of the American Philosophical Society, v. 30, p. 1–510, https://doi.org/10.2307/1005521.

Maxwell, R.A., Lonsdale, J.T., Hazzard, R.T., and Wilson, J.A., 1967, Geology of Big Bend National Park, Brewster County, Texas: University of Texas Bureau of Economic Geology, Publication 6711, 320 p.

McDowell, F.W., Roldan-Quintana, J., and Connelly, J.N., 2001, Duration of Late Cretaceous-early Tertiary magmatism in east-central Sonora, Mexico: Geological Society of America Bulletin, v. 113, no. 4, p. 521–531, https://doi.org/10.1130/0016-7606(2001)113<0521:DOLCET>2.0.CO;2.

Mebrouk, F., Tabuce, R., Cappetta, H., and Feist, M., 2009, Charophytes from the Cretaceous/Paleocene of Middle Atlas (Morocco): Systematic and biochronologic implications: Revue de Micropaleontologie, v. 52, p. 131–139, https://doi.org/10.1016/j.revmic.2007.08.003.

Miall, A.D., 1996, The Geology of Fluvial Deposits—Sedimentary Facies, Basin Analysis and Petroleum Geology: Berlin, Springer-Verlag, 582 p.

Middleton, G.V., and Hampton, M.A., 1973, Sediment gravity flows: Mechanics of flow and deposition, *in* Middleton, G.V., and Bouma, A., eds., Turbidites and Deep Water Sedimentation: Los Angeles, Society of Economic Paleontologists and Mineralogists, Pacific Section, p. 1–38.

Miller, B.A., and Juilleret, J., 2020, The colluvium and alluvium problem: Historical review and current state of definitions: Earth-Science Reviews, v. 209, https://doi.org/10.1016/j.earscirev.2020.103316.

Müller, A., van den Kerkhof, A.M., Behr, H.-J., Kronz, A., and Koch-Müller, M., 2009, The evolution of late-Hercynian granites and rhyolites documented by quartz—A review: Earth and Environmental Science Transactions of the Royal Society of Edinburgh, v. 100 (Special Issue 1–2), p. 185–204.

Musacchio, E.A., 2000, Biostratigraphy and biogeography of Cretaceous charophytes from South America: Cretaceous Research, v. 21, p. 211–220, https://doi.org/10.1006/cres.1999.0197.

Nichols, D.J., and Johnson, K.R., 2008, Plants and the K-T Boundary: Cambridge, UK, Cambridge University Press, 292 p, https://doi.org/10.1017/CBO9780511535536.

Nordt, L., Atchley, S., and Dworkin, S., 2003, Terrestrial evidence for two greenhouse events in the latest Cretaceous: GSA Today, v. 13, no. 12, p. 4–9, https://doi.org/10.1130/1052-5173(2003)013<4:TEFTGE>2.0.CO;2.

Nordt, L., Dworkin, S., and Atchley, S., 2011, Ecosystem response to soil biogeochemical behavior during the Late Cretaceous and early Paleocene within the western interior of North America: Geological Society of America Bulletin, v. 123, p. 1745–1762, https://doi.org/10.1130/B30365.1.

O'Campo, A.C., Pope, K.O., and Fischer, A.G., 1996, Ejecta blanket deposits of the Chicxulub Crater from Albion Island, Belize, *in* Ryder, G., Fastovsky, D., and Gartner, S., eds., The Cretaceous–Tertiary Event and Other Catastrophes in Earth History: Geological Society of America Special Paper 307, p. 75–88, https://doi.org/10.1130/0-8137-2307-8.75.

Olsson, R.K., and Liu, C., 1993, Controversies on the placement of Cretaceous–Paleogene boundary and the K/P mass extinction of planktonic foraminifera: Palaios, v. 8, p. 127–139, https://doi.org/10.2307/3515167.

Osborn, H.F., and Earle, C., 1895, Fossil mammals of the Puerco beds: American Museum of Natural History Bulletin 7, 70 p.

Peck, R.E., and Forester, R.M., 1979, The genus *Platychara* from the western hemisphere: Review of Palaeobotany and Palynology, v. 28, p. 223–236, https://doi.org/10.1016/0034-6667(79)90011-3.

Peck, R.E., and Reker, C.C., 1948, Eocene Charophyta from North America: Journal of Paleontology, v. 22, p. 85–90.

Rapp, S.D., MacFadden, B.J., and Schiebout, J.A., 1983, Magnetic polarity stratigraphy of the early Tertiary Black Peaks Formation, Big Bend National Park, Texas: The Journal of Geology, v. 91, p. 555–572, https://doi.org/10.1086/628804.

Renne, P.R., Deino, A.L., Hilgen, F.J., Kuiper, K.F., Mark, D.F., Mitchell, W.S., Morgan, L.E., Mundil, R., and Smit, J., 2013, Time scales of critical events around the Cretaceous–Paleogene boundary: Science, v. 339, p. 684–687, https://doi.org/10.1126/science.1230492.

Rigby, J.K., Jr., 1980, Swain quarry of the Fort Union Formation, middle Paleocene (Torrejonian), Carbon County, Wyoming, geologic setting and mammalian fauna: Ecological Monographs, v. 3, p. 1–179.

Riveline, J., Berger, J.P., Feist, M., Martin-Closas, C., Schudack, M., and Soulie-Marsche, I., 1996, European Mesozoic–Cenozoic charophyte biozonation: Bulletin de la Société Géologique de France, v. 167, p. 453–468.

Schiebout, J.A., 1974, Vertebrate paleontology and paleoecology of Paleocene Black Peaks Formation, Big Bend National Park, Texas: Texas Memorial Museum Bulletin 24, 88 p.

Schiebout, J.A., Rigsby, C.A., Rapp, S.D., Hartnell, J.A., and Standhardt, B.R., 1987, Stratigraphy of the Cretaceous–Tertiary and Paleocene–Eocene transition rocks of Big Bend National Park, Texas: The Journal of Geology, v. 95, p. 359–375, https://doi.org/10.1086/629135.

Schiebout, J.A., Rigsby, C.A., Standhardt, B.R., Rapp, S.D., and Hartnell, J.A., 1988, Stratigraphy of the Cretaceous–Tertiary and Paleocene–Eocene transition rocks of Big Bend National Park, Texas—A reply: The Journal of Geology, v. 96, p. 631–634, https://doi.org/10.1086/629259.

Schmidt, D.R., 2009, Stable isotope geochemistry of Upper Cretaceous and Paleocene strata in Big Bend National Park, Texas [Ph.D. thesis]: Lubbock, Texas Tech University, 202 p.
Schoch, R.M., 1986, Systematics, functional morphology and macroevolution of the extinct mammalian Order Taeniodonta: Yale University, Peabody Museum of Natural History Bulletin 42, 307 p.
Schulte, P., Alegret, L., Arenillas, I., Arz, J.A., Barton, P.J., Bown, P.R., Bralower, T.J., Christeson, G.L., Claeys, P., Cockell, C.S., Collins, G.S., Deutsch, A., Goldin, T.J., Goto, K., Grajales-Nishimura, J.M., Grieve, R.A., Gulick, S.P., Johnson, K.R., Kiessling, W., Koeberl, C., Kring, D.A., Macleod, K.G., Matsui, T., Melosh, J., Montanari, A., Morgan, J.V., Neal, C.R., Nichols, D.J., Norris, R.D., Pierazzo, E., Ravizza, G., Rebolledo-Vieyra, M., Reimold, W.U., Robin, E., Salge, T., Speijer, R.P., Sweet, A.R., Urrutia-Fucugauchi, J., Vajda, V., Whalen, M.T., and Willumsen, P.S., 2010, The Chicxulub asteroid impact and mass extinction at the Cretaceous-Paleogene boundary: Science, v. 327, p. 1214–1218, https://doi.org/10.1126/science.1177265.
Selby, M.J., 1993, Hillslope Materials and Processes (2nd edition): Oxford, UK, Oxford University Press, 264 p.
Shelley, S.L., Williamson, T.E., and Brusatte, S.L., 2018, The osteology of *Periptychus carinidens*: A robust, ungulate-like placental mammal (Mammalia: Periptychidae) from the Paleocene of North America: PLoS One, v. 13, no. 7, https://doi.org/10.1371/journal.pone.0200132.
Simpson, G.G., 1935, The Tiffany fauna, upper Paleocene. III—Primates, Carnivora, Condylarthra, and Amblypoda: American Museum of Natural History, Novitates 817, 28 p.
Simpson, G.G., 1937, The Fort Union of the Crazy Mountain field, Montana and its mammalian fauna: U.S. National Museum Bulletin, v. 169, 287 p.
Sloan, R.E., Rigby, J.K., Van Valen, L.M., and Gabriel, D., 1986, Gradual dinosaur extinction and simultaneous ungulate radiation in the Hell Creek formation: Science, v. 232, p. 629–633, https://doi.org/10.1126/science.232.4750.629.
Smit, J., Roep, Th.B., Alvarez, W., Claeys, P., Grajales-Nishimura, J.M., and Bermudez, J., 1996, Coarse grained, clastic sandstone complex at the K/T boundary around the Gulf of Mexico: Deposition by tsunami waves induced by the Chicxulub impact?, *in* Ryder, G., Fastovsky, D., and Gartner, S., eds., Cretaceous–Tertiary Event and Other Catastrophes in Earth History: Geological Society of America Special Paper 307, p. 151–182, https://doi.org/10.1130/0-8137-2307-8.151.
Smyth, H.R., Hall, R., and Nichols, G.J., 2008, Significant volcanic contribution to some quartz-rich sandstones, East Java, Indonesia: Journal of Sedimentary Research, v. 78, p. 335–356, https://doi.org/10.2110/jsr.2008.039.
Stacey, J.S., and Kramers, J.D., 1975, Approximation of terrestrial lead isotope evolution by a two-stage model: Earth and Planetary Science Letters, v. 26, p. 207–221, https://doi.org/10.1016/0012-821X(75)90088-6.
Standhardt, B.R., 1986, Vertebrate paleontology of the Cretaceous/Tertiary transition of Big Bend National Park, Texas [Ph.D. thesis]: Baton Rouge, Louisiana State University, 298 p.
Stinnesbeck, W., Barbarin, J.M., Keller, G., Lopez-Oliva, J.G., Pivnik, D.A., Lyons, J.B., Officer, C.B., Adatte, T., Graup, G., and Rocchia, R., 1993, Deposition of channel deposits near the Cretaceous-Tertiary boundary in northeastern Mexico: Catastrophic or “normal” sedimentary deposits?: Geology, v. 21, p. 797–800, https://doi.org/10.1130/0091-7613(1993)021<0797:DOCDNT>2.3.CO;2.
Stöffler, D., and Langenhorst, F., 1994, Shock metamorphism of quartz in nature and experiment: 1. Basic observation and theory: Meteoritics, v. 29, p. 155–181, https://doi.org/10.1111/j.1945-5100.1994.tb00670.x.
Straight, W.H., 1996, Stratigraphy and paleontology of the Cretaceous–Tertiary boundary, Big Bend National Park, Texas [M.S. thesis]: Lubbock, Texas Tech University, 102 p.
Sullivan, R.M., Lucas, S.G., and Braman, D.R., 2005, Dinosaurs, pollen, and the Cretaceous–Tertiary boundary in the San Juan Basin, New Mexico, *in* Lucas, S.G., Zeigler, K.E., Lueth, V.W., and Owen, D.E., eds., Geology of the Chama Basin: New Mexico Geological Society 56th Field Conference Guidebook, p. 395–407.
Taylor, L.H., 1984, Review of Torrejonian mammals from the San Juan Basin, New Mexico [Ph.D. thesis]: Tucson, University of Arizona, 553 p.
Thewissen, J.G., 1990, Evolution of Paleocene and Eocene Phenacodontidae (Mammalia, Condylarthra): University of Michigan Papers on Paleontology 29, 107 p.
Tomlinson, S.L., 1997, Late Cretaceous and early Tertiary turtles from the Big Bend region, Brewster County, Texas [Ph.D. thesis]: Lubbock, Texas Tech University, 194 p.
Turner, K.J., Berry, M.E., Page, W.R., Lehman, T.M., Bohannon, R.G., Scott, R.B., Miggins, D.P., Budahn, J.R., Cooper, R.W., Drenth, B.J., Anderson, E.D., and Williams, V.S., 2011, Geologic Map of Big Bend National Park, Texas: U.S. Geological Survey, Scientific Investigations Map No. 3142, scale 1:75,000, pamphlet 84 p.
Van Valen, L., 1978, The beginning of the age of mammals: Evolutionary Theory, v. 4, p. 45–80.
Vermeesch, P., 2018, IsoplotR: A free and open toolbox for geochronology: Geoscience Frontiers, v. 9, p. 1479–1493, https://doi.org/10.1016/j.gsf.2018.04.001.
Vines, C.M., 2000, Mineralogy and geochemistry of paleosols in the Javelina and Black Peaks Formations (Late Cretaceous–Paleocene) Big Bend National Park, Texas [M.S. thesis]: Lubbock, Texas Tech University, 114 p.
West, R.M., 1976, The North American Phenacodontidae (Mammalia, Condylarthra): Milwaukee Public Museum: Contributions in Biology and Geology, v. 6, p. 1–78.
Wheeler, E.A., 1991, Paleocene dicotyledonous trees from Big Bend National Park, Texas: Variability in wood types common in the Late Cretaceous and early Tertiary, and ecological inferences: American Journal of Botany, v. 78, p. 658–671, https://doi.org/10.1002/j.1537-2197.1991.tb12590.x.
White, P.D., and Schiebout, J.A., 2003, Paleogene paleosols of Big Bend National Park, Texas, *in* Wing, S.L., Gingerich, P.D., Schmitz, B., and Thomas, E., eds., Causes and Consequences of Globally Warm Climates in the Early Paleogene: Geological Society of America Special Paper 369, p. 537–550, https://doi.org/10.1130/0-8137-2369-8.537.
White, P.D., and Schiebout, J.A., 2008, Paleogene paleosols and changes in pedogenesis during the initial Eocene thermal maximum: Big Bend National Park, Texas, USA: Geological Society of America Bulletin, v. 120, p. 1347–1361, https://doi.org/10.1130/B25987.1.
Wick, S.L., and Lehman, T.M., 2014, A complete titanosaur femur from West Texas with comments regarding hindlimb posture: Cretaceous Research, v. 49, p. 39–44, https://doi.org/10.1016/j.cretres.2014.02.003.
Wiest, L.A., Lukens, W.E., Peppe, D.J., Driese, S.G., and Tubbs, J., 2018, Terrestrial evidence for the Lilliput effect across the Cretaceous–Paleogene (K-Pg) boundary: Palaeogeography, Palaeoclimatology, Palaeoecology, v. 491, p. 161–169, https://doi.org/10.1016/j.palaeo.2017.12.005.
Williamson, T.E., 1996, The beginning of the age of mammals in the San Juan Basin, New Mexico: Biostratigraphy and evolution of Paleocene mammals of the Nacimiento Formation: New Mexico Museum of Natural History and Science, Bulletin 8, 141 p.
Williamson, T.E., and Lucas, S.G., 1992, Stratigraphy and mammalian biostratigraphy of the Paleocene Nacimiento Formation, southern San Juan Basin, New Mexico: New Mexico Geological Society Guidebook, 43rd Field Conference, p. 265–296.
Wilson, G.P., Clemens, W.A., Horner, J.R., and Hartman, J.H., 2014, Through the End of the Cretaceous in the Type Locality of the Hell Creek Formation in Montana and Adjacent Areas: Geological Society of America Special Paper 503, 392 p., https://doi.org/10.1130/SPE503.
Zhang, X., Pease, V., Skogseid, J., and Wohlgemuth-Ueberwasser, C., 2016, Reconstruction of tectonic events on northern Eurasia margin of the Arctic from U-Pb detrital zircon provenance investigations of late Paleozoic to Mesozoic sandstones in southern Taimyr Peninsula: Geological Society of America Bulletin, v. 128, no. 1–2, p. 29–46, https://doi.org/10.1130/B31241.1.